FRIEDRICH-SCHILLER-UNIVERSITÄT JENA
PHYSIKALISCH-ASTRONOMISCHE-FAKULTÄT

FRIEDRICH-SCHILLER-
UNIVERSITÄT
JENA

WINTERSEMESTER 2021/2022

Thinfilm optics

DR. OLAF STENZEL

LaTeX-Satz und Design von Martin Beyer

Contents

1 Introduction

Why do we do Thinfilm Optics? In order to describe the transmittance and reflectance of a surface, we use FRESNEL's equations where we define transmittance and reflectance as

$$R := \frac{I_r}{I_e} \quad \text{and} \quad T := \frac{I_t}{I_e}, \tag{1.1}$$

where I_t and I_r are the transmitted and reflected intensity and I_e is the incident (german. einfallend) intensity. For glass ($n = 1.5$) and normal incidence we find a reflectivity of $R = 4\,\%$. For many surfaces the transmittance is much more reduced. Thus, there is a need in manipulating the reflectance. In order to enhance/reduce the reflectance we need to establish a high/anti reflective coating.

1.1 Symbols, Definitions, Conventions

In this script we use some special conventions which are listed in the following:

- λ, c - wavelength/speed of light in vacuum
- ω - angular frequency ($\omega = \frac{2\pi c}{\lambda} = 2\pi c\nu$)
- ν - wave number $\nu \equiv \frac{1}{\lambda}$
- E - photon energy $E = \hbar\omega = hc\nu$.

It should be mentioned that ν is not the frequency but the wavenumber with units of inverse metres. As a rule of thumb we can say that wavenumber and energy can be related as

$$1\,\text{eV} \mathrel{\widehat{=}} 8065\,\frac{1}{\text{cm}} \quad \text{and} \quad \lambda[\mu\text{m}] \mathrel{\widehat{=}} \frac{1.24}{E[\text{eV}]}. \tag{1.2}$$

The different spectral regions of electromagnetic radiation are summarized in table 1.

Table 1: Spectral regions of light.

name		λ	ν, E
microwave	MW	$> 1\,\text{mm}$	
terahertz	THz	0,1 mm…1 mm	
far infrared	FIR	50 µm …1 mm	10/cm…200/cm
mid infrared	MIR	2,5 µm…50 µm	200/cm…4000/cm
near infrared	NIR	0,7 µm…2,5 µm	4000/cm…14 300/cm
visual	VIS	0,4 µm…0,7 µm	1,8 eV…3,1 eV
ultraviolet	UV	10 nm…400 nm	3,1 eV…125 eV
x-rays	X	$< 10\,\text{nm}$	

We also want to use the convention that the electric field $\boldsymbol{E}$ is defined as

$$\begin{aligned}\boldsymbol{E}(\boldsymbol{r},t) &= \boldsymbol{E}_{00}\cos(\omega t - \boldsymbol{k}\cdot\boldsymbol{r} + \delta_0) \\ &= \frac{\boldsymbol{E}_{00}}{2}\mathrm{e}^{-\mathrm{i}\delta_0}\mathrm{e}^{-\mathrm{i}(\omega t - \boldsymbol{k}\cdot\boldsymbol{r})} + \text{c.c.}\end{aligned} \tag{1.3}$$

Thus, the complex refractive index $\hat{n}$ is given as $\hat{n} = n + \mathrm{i}k$.

1.2 General problem of light-matter interaction

The general problem of the interaction of light and matter can be visualized in the following sketch:

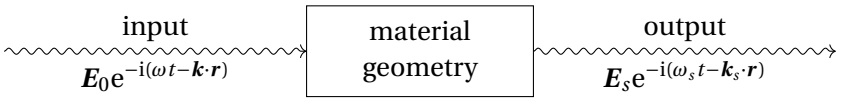

Figure 1: Scheme of light-matter interaction

There are two different approaches to tackle this problem:

- Forward search: For a given input and system one concludes the output. This leads to a *design taks*, where we have to find our dream material. For a design task a solution is not guaranteed, however, many solutions are helpful in practice.
- Reverse search: For a given input and output one concludes on system properties. This leads to a *characterization task*, where the output is a measured quantity. For a characterization task a solution must exist, however, for the case of several solution we have to identify the physically meaningful one.

2 Material equations in linear optics

2.1 Linear dielectric susceptibility

At first, we want to discuss the linear dielectric susceptibility. For a homogeneous, isotropic and non-magnetic media we can define the dielectric displacement vector as

$$\boldsymbol{D} = \varepsilon_0 \boldsymbol{E} + \boldsymbol{P} \quad \text{with} \quad \boldsymbol{P}(t) = \varepsilon_0 \int_0^\infty \chi(\tau) \boldsymbol{E}(t-\tau)\,\mathrm{d}\tau\,, \tag{2.1}$$

where $\boldsymbol{P}(t)$ is the polarization and $\chi(\tau)$ the response function (real) containing the material information. In frequency space we can relate polarization and electric field via

$$\boldsymbol{P}_0 = \chi(\omega)\boldsymbol{E}_0 \quad \text{with} \quad \chi(\omega) = \frac{1}{\sqrt{2\pi}} \int_0^\infty \chi(\tau) \mathrm{e}^{-\mathrm{i}\omega\tau}\,\mathrm{d}\tau\,. \tag{2.2}$$

The response function $\chi(\omega)$ is then ω-dependent and complex. Now we want to relate the dielectric displacement with the electric field

$$\boldsymbol{D}_0 = \varepsilon_0 \varepsilon(\omega)\boldsymbol{E}_0 \quad \text{with} \quad \varepsilon(\omega) = 1 + \chi(\omega) \quad \Rightarrow \quad \hat{n} = \sqrt{\varepsilon(\omega)} = n + \mathrm{i}k. \tag{2.3}$$

Furthermore we can introduce a damping coefficient α in the material as

$$\alpha = 4\pi\nu k = \frac{2\omega}{c} k. \tag{2.4}$$

2.2 Commonly used dispersion models

In order to model the frequency behavior of the refractive index we want to look at the polarizability $\boldsymbol{p} = \alpha \boldsymbol{E}$. In the classical Lorentz oscillator model we find

$$\alpha(\omega) = \frac{q^2}{\varepsilon_0 m} \frac{1}{\omega_0^2 - \omega^2 - 2\mathrm{i}\omega\gamma}. \tag{2.5}$$

Now we can relate the macroscopic dielectric function with the microscopic polarizability using the relation

$$\frac{\varepsilon - 1}{\varepsilon + 2} = \frac{N\alpha}{3} \quad \text{Clausius Mosotti relation.} \tag{2.6}$$

We can derive this equation by looking at the macroscopic polarization as a function of the local electric field

$$\boldsymbol{P} = N\boldsymbol{p}_{\text{ind}} = N\alpha \boldsymbol{E}_{\text{local}}. \tag{2.7}$$

The local electric field strength at the atom is the superposition of the external field $\boldsymbol{E}$ and a polarization field $\boldsymbol{E}_L$ (Lorentz field) created by polarization charges on the surface on a sphere around the atom. This field is given by

$$\boldsymbol{E}_L = \frac{\boldsymbol{P}}{3\varepsilon_0} = \frac{(\varepsilon-1)\varepsilon_0}{3\varepsilon_0}\boldsymbol{E} \quad \Rightarrow \quad \boldsymbol{E}_{\text{local}} = \left(1+\frac{\varepsilon-1}{3}\right)\boldsymbol{E} = \frac{\varepsilon+2}{3}\boldsymbol{E}. \tag{2.8}$$

Substituting this into equation (2.7) and using $\boldsymbol{P} = \varepsilon_0(\varepsilon-1)\boldsymbol{E}$ we find

$$\boldsymbol{P} = \varepsilon_0(\varepsilon-1)\boldsymbol{E} = N\alpha\frac{\varepsilon+2}{3}\boldsymbol{E} \quad \Rightarrow \quad \frac{\varepsilon-1}{\varepsilon+2} = \frac{N\alpha}{3}. \tag{2.9}$$

From that we can deduce the dielectric function as

$$\varepsilon(\omega) = 1+\frac{N\alpha}{1-\frac{N\alpha}{3}} = 1+\frac{\frac{Nq^2}{\varepsilon_0 m}}{\tilde{\omega}_0^2-\omega^2-2\mathrm{i}\omega\gamma} \quad \text{with} \quad \tilde{\omega}_0^2 = \omega_0^2-\frac{\omega_p^2}{3}. \tag{2.10}$$

Here we defined the plasma frequency ω_p as

$$\omega_p^2 = \frac{Nq^2}{\varepsilon_0 m}. \tag{2.11}$$

In general we can write the dielectric function as a free space part and a bounded part, influenced by the oscillator strengths and resonances of the bound atoms

$$\varepsilon(\omega) = 1-\frac{\omega_{p,\text{free}}^2}{\omega^2-2\mathrm{i}\omega\gamma}+\omega_{p,\text{bound}}^2\sum_i\frac{f_i}{\omega_{0,i}^2-\omega^2-2\mathrm{i}\omega\gamma_i}. \tag{2.12}$$

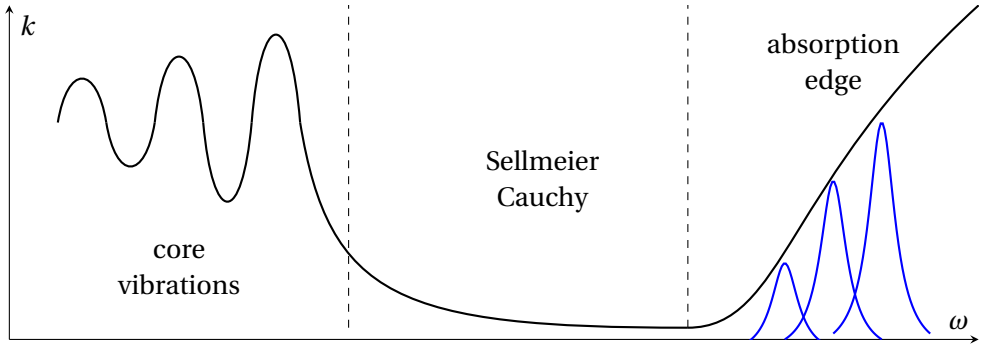

Figure 2: typical absorption behavior in dielectrics.

Tauc-Lorentz-model

This dispersion model was developed in 1998 by Jellison. Here we combine the Tauc relation

$$\mathrm{Im}(\varepsilon) \propto \frac{(\hbar\omega-E_{\text{gap}})^2}{\omega^2}\Theta(\hbar\omega-E_{\text{gap}}) \tag{2.13}$$

(where Θ describes the HEAVISIDE function) with the Lorentz model mentioned in equation (2.7). The Tauc relation gives us zero absorption if the wavelength of the photons is below the optical gap of the medium. The combined model is then

$$\mathrm{Im}(\varepsilon) \propto \frac{(\hbar\omega-E_{\text{gap}})^2}{\omega}\frac{1}{(\omega_0-\omega)^2+4\omega^2\gamma^2}\Theta(\hbar\omega-E_{\text{gap}}). \tag{2.14}$$

The Tauc-Lorentz curve is compared to the Lorentz-model in figure 3.

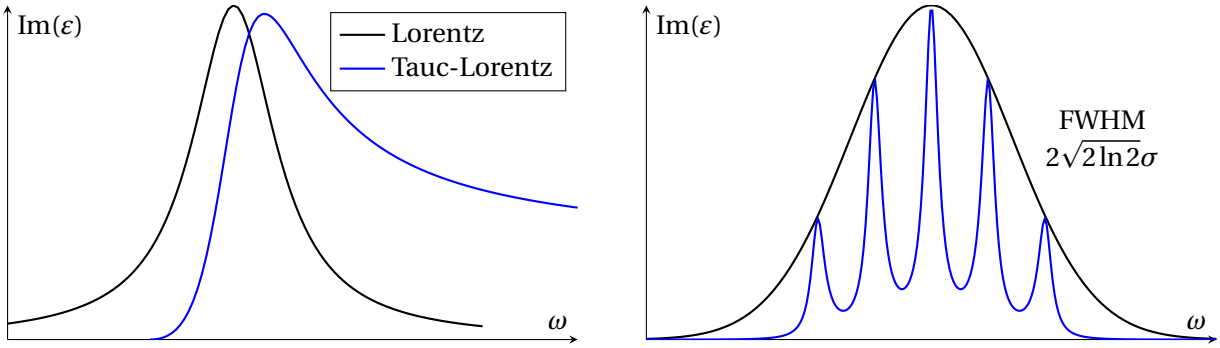

Figure 3: Left:Comparison of the absorption ($\mathrm{Im}\,\varepsilon$) for the Lorentz model and the Lorentz-Tauc model. Right: Brendel model. The Gaussian envelope is modulated by several Lorentzian lines.

Brendel model

Another class of models makes use of inhomogeneous broadening effects (e. g. Doppler shift). Now we replace the sum in equation (2.12) with an integral and write

$$\varepsilon(\omega) = 1 + \int_{-\infty}^{\infty} w(\xi) \frac{\omega_p^2}{\xi^2 - \omega^2 - 2\mathrm{i}\omega\gamma} \,\mathrm{d}\xi \,. \tag{2.15}$$

The most popular of such models is the Brendel model (1992) where we have

$$\varepsilon(\omega) = 1 + \frac{1}{\sqrt{2\pi}} \int_{-\infty}^{\infty} \exp\left(\frac{(\xi - \bar{\omega}_0)^2}{2\sigma^2}\right) \frac{\omega_p^2}{\xi^2 - \omega^2 - 2\mathrm{i}\omega\gamma} \,\mathrm{d}\xi \,. \tag{2.16}$$

This function describes a broad Gaussian curve centered at $\bar{\omega}_0$ with several Lorentzian's inside. We can now distinguish three different limiting cases:

- $\gamma \gg \sigma$: Envelope collapses into a single Lorentzian line.
- $\gamma \ll \sigma$: The Lorentzians become Delta-functions → Gaussian line.
- $\gamma \approx \sigma$: We obtain a Voigt line.

In order to merge the idea of inhomogeneous broadening with possibility to model a threshhold for the dielectric function we arrive at the β-distributed oscillator model published by Wilbrandt in 2017

$$W(\xi) \propto \begin{cases} (\xi - \omega_a)^{A-1} (\omega_b - \xi)^{B-1} & \xi \in (\omega_a, \omega_b), A, B > 0 \\ 0 & \xi \notin (\omega_a, \omega_b) \end{cases} . \tag{2.17}$$

We can combine asymmetry with absorption edge modeling. This is the most flexible model, however, we have a total of six free parameters ($A, B, \omega_a, \omega_b, \gamma$, global proportionality constant).

3 Impact of real structures

3.1 Material mixtures: simplest model

We now want to consider mixtures of different materials. The simmplest way to model such a mixture is a *binary mixture* of two materials with corresponding dielectric constants ε_1 and ε_2 with a volume filling factor $p_1 = \frac{V_1}{V}$ and $p_2 = \frac{V_2}{V}$, where V is the total volume of the material. As a first guess we might assume that the total dielectric constant may be

$$\varepsilon \stackrel{?}{=} p_1\varepsilon_1 + p_2\varepsilon_2. \tag{3.1}$$

In order to check if this is generally true we perform a Gedankenexperiment of a binary mixtures with thin layers of alternating material. If we place this dielectric into a capacitor the total capacity will be

$$C = \varepsilon_0\varepsilon\frac{A}{d}. \tag{3.2}$$

If we align the material layers perpendicular to the capacitor plates, we can assume this to

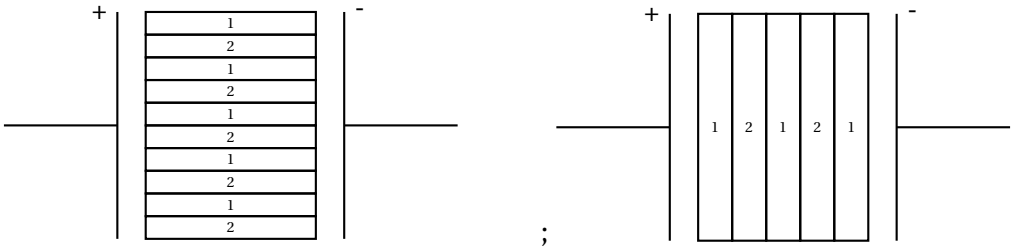

Figure 4: Left: Horizontal arrangement. The total capacity can be obtained by adding the capacities of every small layer. We have a parallel connection of capacitors.
Right: Vertical arrangement. We can model this as a series connection of capacitors.

be a parallel connection of several capacitors

$$C = C_1 + C_2 + C_1 + \ldots \quad \Rightarrow \quad \varepsilon = p_1\varepsilon_1 + p_2\varepsilon_2 = \varepsilon_\parallel. \tag{3.3}$$

However, if we align the layers parallel to the capacitor plates, we instead assume a series connection of capacitors

$$\frac{1}{C} = \frac{1}{C_1} + \frac{1}{C_2} + \ldots \quad \Rightarrow \quad \frac{1}{\varepsilon} = \frac{p_1}{\varepsilon_1} + \frac{p_2}{\varepsilon_2} = \frac{1}{\varepsilon_\perp} \Rightarrow \varepsilon_\perp = \frac{\varepsilon_1\varepsilon_2}{p_1\varepsilon_2 + p_2\varepsilon_1}. \tag{3.4}$$

We observe that geometry of the material does matter. For a small mixing like $p_1 \ll p_2$ or $p_2 \ll p_1$ the linear superposition $\varepsilon_\parallel$ is a reasonable approximation.

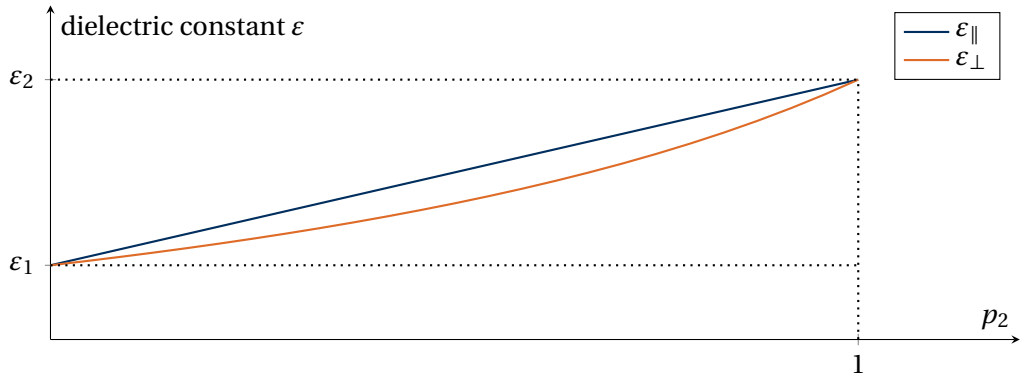

Figure 5: Dielectric constant ε of a binary structure for a parallel and perpendicular geometry. The curves $\varepsilon_\parallel$ and $\varepsilon_\perp$ are called WIENER bounds. The dielectric constant for different structures lies in the area between these two bounds.

Lorentz-Lorenz mixing model

In this model we generalize the Clausius-Mosotti relation for a material with different polarizabilities

$$\frac{\varepsilon-1}{\varepsilon+2}=\frac{1}{3}\sum_i N_i\alpha_i. \tag{3.5}$$

For a single material in the mixture we still have

$$\frac{N_0\alpha_i}{3}=\frac{\varepsilon_i-1}{\varepsilon_i+2}\Rightarrow\alpha_i=\frac{3}{N_0}\frac{\varepsilon_i-1}{\varepsilon_i+2}. \tag{3.6}$$

If we now insert (3.6) into equation (3.5) we obtain

$$\frac{\varepsilon-1}{\varepsilon+2}=\sum_i \underbrace{\frac{N_i}{N_0}}_{p_i}\frac{\varepsilon_i-1}{\varepsilon_i+2} \quad\Rightarrow\quad \boxed{\frac{\varepsilon-1}{\varepsilon+2}=\sum_i p_i\frac{\varepsilon_i-1}{\varepsilon_i+2}} \quad \text{with} \quad E_{\text{local}}=\boldsymbol{E}+\boldsymbol{E}_L \tag{3.7}$$

For a binary mixture we find

$$\frac{\varepsilon-1}{\varepsilon+2}=(1-p_2)\frac{\varepsilon_1-1}{\varepsilon_1+2}+p_2\frac{\varepsilon_2-1}{\varepsilon_2+2}. \tag{3.8}$$

For a thinsolid film we may assume that material 1 consists of pores and material 2 is the solid material. Then we call $p_1=1-p_2=1-p$ the *porosity* of the thinfilm and $p_2=p$ the *packing density*. If the pores are empty we have $\varepsilon_1=1$ which implies

$$\frac{n^2-1}{n^2+2}=p\frac{n_b^2-1}{n_b^2+2}. \tag{3.9}$$

We observe that for increasing packing density (and corresponding mass density ρ) the refractive index increases linearly aswell $\frac{\partial n}{\partial\rho}>0$.

3.2 Columnar structure

A closer description of reality is the columnar structure. However, we need a generalization of the Lorentz-Lorenz formula to a cylindrical geometry. In contrast to equation (2.8) the local electric field in a cylindrical geometry is

$$\boldsymbol{E}_{\text{local}} = \boldsymbol{E} + \frac{\boldsymbol{P}}{2\varepsilon_0} = \frac{\varepsilon+1}{2}\boldsymbol{E}. \tag{3.10}$$

Analogous to equation (2.9) we arrive at

$$\boldsymbol{P} = \varepsilon_0(\varepsilon-1)\boldsymbol{E} = N\alpha\frac{\varepsilon+1}{2}\boldsymbol{E} \quad \Rightarrow \quad \frac{\varepsilon-1}{\varepsilon+1} = \frac{N\alpha}{2}. \tag{3.11}$$

For a material mixture we can again write this as

$$\frac{n^2-1}{n^2+1} = (1-p)\frac{n_0^2-1}{n_0^2+1} + p\frac{n_b^2-1}{n_b^2+1}. \tag{3.12}$$

For room temperature the pores may be filled by water ($n_0^2 = 1.77$) whereas at $T > 100\,^\circ$C they are filled with air ($n_0^2 = 1$). This means the refractive index of a thin film is typically falling for rising temperatures

$$n(T = 100\,^\circ\text{C}) < n(T = 23\,^\circ\text{C}), \quad \frac{\partial n}{\partial T} < 0. \tag{3.13}$$

This thermal shift, however, is influenced by the porosity of the thin film.

3.3 Simple treatment of mixtures with metals

We now want to apply the two different bounds for a material mixture

$$\begin{aligned} \varepsilon_\parallel &= p_1\varepsilon_1 + p_2\varepsilon_2, \\ \varepsilon_\perp &= \frac{\varepsilon_1\varepsilon_2}{p_1\varepsilon_2 + p_2\varepsilon_1} \quad \text{with} \quad p_1 + p_2 = 1 \end{aligned} \tag{3.14}$$

on a metal. We consider a dielectric ($\varepsilon > 0$) and a metal $\varepsilon < 0$ which can be described by the Lorentz model (with $\omega_0 = 0$)

$$\varepsilon = 1 - \frac{\omega_p^2}{\omega^2 + 2\mathrm{i}\omega\gamma}\bigg|_{\omega\gg\gamma} = 1 - \frac{\omega_p^2}{\omega^2}. \tag{3.15}$$

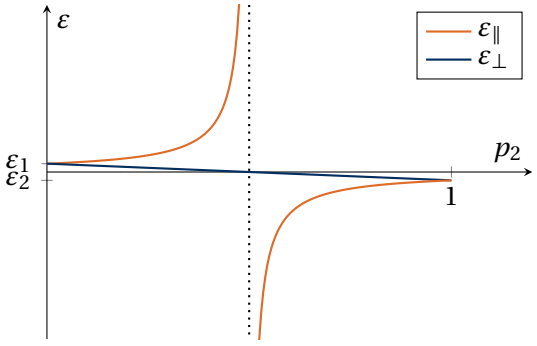

Figure 6: dielectric function of a metal.

Example: metal island film

Figure 7: Metal island film.

As a simplest system we assume a simple island film at normal incidence. Over the dimension of the extension of a single metal island we can assume that the electric field is homogeneous if the diameter of the metal islands is $d \ll \lambda$. The surrounding medium should be air $\varepsilon_1 = 1$ and the metal has $\varepsilon_2 = \varepsilon_m$. We are searching for frequencies where the mixture has a strong response ($\varepsilon \to \infty$). Then we find

$$\frac{\varepsilon - 1}{\varepsilon + 2} = p\frac{\varepsilon_m - 1}{\varepsilon_m + 2} \quad \Rightarrow 1 = p\frac{\varepsilon_m - 1}{\varepsilon_m + 2} \quad \Rightarrow \varepsilon_m = -\frac{p+2}{1-p}. \tag{3.16}$$

Since we are at resonance we can write

$$\varepsilon_m = -\frac{p+2}{1-p} \stackrel{!}{=} 1 - \frac{\omega_p^2}{\omega^2} \quad \Rightarrow \quad \omega = \sqrt{1-p}\frac{\omega_p}{\sqrt{3}}. \tag{3.17}$$

For $p \to 0$ we find $\omega \to \omega_p/\sqrt{3}$ which is the resonance frequency of a single small metal in air. This coincides with the expression of a localized surface plasmon excitation in a small metal sphere. If we have a nonzero filling factor p the resonant frequency (3.17) shifts to the visible spectral range. Thus the metal island film may appear colored. Only for a full metal film ($p \to 1$) we would have $\omega_{\text{res}} = 0$ as we always assume in the Lorentz model for metals.

Let us introduce a modification in the system, that the metal islands are not surrounded in air but in a dielectric material $\varepsilon_1 = \varepsilon_h$ (host). Then the Lorentz-Lorenz equation states

$$\begin{aligned} \frac{\varepsilon - 1}{\varepsilon + 2} &= p\frac{\varepsilon_m - 1}{\varepsilon_m + 2} + (1-p)\frac{\varepsilon_h - 1}{\varepsilon_h + 2} \quad \text{with} \quad \varepsilon \to \infty \\ \underbrace{1 - (1-p)\frac{\varepsilon_h - 1}{\varepsilon_h + 2}}_{\text{finite}} &= p\frac{\varepsilon_m - 1}{\varepsilon_m + 2}. \end{aligned} \tag{3.18}$$

Again, for a single metal sphere we assume $p \to 0$, then

$$\frac{\varepsilon_m - 1}{\varepsilon_m + 2} \to \infty \Rightarrow \varepsilon_m + 2 = 0 \Rightarrow 3 - \frac{\omega_p^2}{\omega^2} = 0 \Rightarrow \omega = \frac{\omega_p}{\sqrt{3}}. \tag{3.19}$$

This means the dielectric constant of a single metal sphere does not depend on the properties of the surrounding medium. However, one would normally expect that for higher ε_h the movement of the charges in the host material would be slower and the resonance frequency would go down. This can also be verified experimentally. Thus, our theory is incomplete.

3.4 General approach to material mixtures

3.4.1 Model calculation: Field in in polarized sphere

We now consider the field in a polarized sphere in electrostatics in order to resolve our problem of before. We assume a quasistatic condition with $\lambda \gg 2R$. If we have a homogeneous field inside the sphere we have

$$\begin{aligned}\varphi_1(\boldsymbol{r}) &= -\boldsymbol{E}_1\boldsymbol{r}\\ \varphi_2(\boldsymbol{r}) &= -\boldsymbol{E}_2\boldsymbol{r} + A \quad \underbrace{\boldsymbol{E}_2\frac{\boldsymbol{r}}{r^3}}_{\text{dipole moment}}\\ &= -\boldsymbol{E}_2\boldsymbol{r}\left(1-\frac{A}{r^3}\right).\end{aligned} \tag{3.20}$$

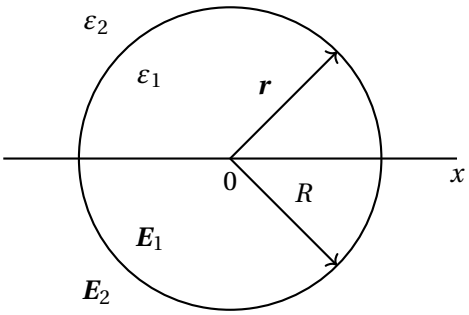

Figure 8: Geometry of a single metal film.

Outside the medium we assume a dipole moement $\varphi = \frac{1}{4\pi\varepsilon_0}\frac{\boldsymbol{d}\cdot\boldsymbol{r}}{r^3}$ where $\boldsymbol{d} \propto \boldsymbol{E}$. At the border the potential should be continuous

$$\varphi_1(R) \stackrel{!}{=} \varphi_2(R) \Rightarrow -E_1 = -E_2\left(1-\frac{A}{r^3}\right) \quad \Rightarrow \quad \frac{A}{R^3} = 1-\frac{E_1}{E_2}. \tag{3.21}$$

Furthermore we demand that the perpendicular component of the dielectric displacement should be continous

$$\begin{aligned}D_{1\perp} = D_{2\perp} \quad &\Rightarrow \quad \varepsilon_0\varepsilon_1 E_1 = \varepsilon_0\varepsilon_2 E_2\left(1+\frac{2A}{R^3}\right)\\ &\Rightarrow \varepsilon_1 E_1 = \varepsilon_2 E_2(1+2-2\frac{E_1}{E_2}) = 3\varepsilon_2 E_2 - 2\varepsilon_2 E_1\\ &\Rightarrow (\varepsilon_1+2\varepsilon_2)E_1 = 3\varepsilon_2 E_2.\end{aligned} \tag{3.22}$$

Finally we arrive at

$$E_2 = \frac{\varepsilon_1+2\varepsilon_2}{3\varepsilon_2}E_1 \tag{3.23}$$

which can be compared to (2.8).

3.4.2 General mixing formula

Let us now imagine a medium that is composed of a host material ε_h and different kind of inclusions ε_j. Now the generalized Lorentz-Lorenz formula states

$$\frac{\varepsilon-\varepsilon_h}{\varepsilon+2\varepsilon_h} = \sum_j p_j \frac{\varepsilon_j-\varepsilon_h}{\varepsilon_j+2\varepsilon_h}. \tag{3.24}$$

Now we raise the question what happens if the inclusions fill the space completely and $\sum_j p_j = 1$ implying that we do not have a host material. There are different approaches:

- *Lorentz-Lorenz mixing approach*: Assume loosely packed materials. We can use this to model small-scale surface roughness

$$\varepsilon_h = 1 \quad \Rightarrow \quad \frac{\varepsilon - 1}{\varepsilon + 2} = \sum_j p_j \frac{\varepsilon_j - 1}{\varepsilon_j + 2} \tag{3.25}$$

- *Maxwell Garnett approach*: The host material acts like one of the mixing partners. This is applied for guest-host systems (metal island films).

$$\varepsilon_h = \varepsilon_{j0} \quad \Rightarrow \quad \frac{\varepsilon - \varepsilon_{j0}}{\varepsilon + 2\varepsilon_{j0}} = \sum_{j \neq j_0} p_j \frac{\varepsilon_j - \varepsilon_h}{\varepsilon_j + 2\varepsilon_h} \Rightarrow \sum_{j \neq j_0} p_j < 1. \tag{3.26}$$

  We can take the Maxwell Garnett model to check, whether or not the single sphere embedded in a dielectric now has a resonance that depends on the optical propertiers of the dielectric:

$$\begin{aligned} \frac{\varepsilon - \varepsilon_h}{\varepsilon + 2\varepsilon_h} = p \frac{\varepsilon_m - \varepsilon_h}{\varepsilon_m + 2\varepsilon_h} \quad \Rightarrow \quad \varepsilon \to \infty \Rightarrow 1 = p \frac{\varepsilon_m - \varepsilon_h}{\varepsilon_m + 2\varepsilon_h} \\ \Rightarrow \varepsilon_m + 2\varepsilon_h = 0 \Rightarrow 1 - \frac{\omega_p^2}{\omega^2} + 2\varepsilon_h = 0 \Rightarrow 1 + 2\varepsilon_h = \frac{\omega_p^2}{\omega_2}. \end{aligned} \tag{3.27}$$

  Then we find

$$\omega = \frac{\omega_p}{\sqrt{1 + 2\varepsilon_h}} \quad \text{for} \quad \varepsilon_h = 1 \Rightarrow \omega = \frac{\omega_p}{\sqrt{3}}. \tag{3.28}$$

  We can see that $\frac{\partial \omega}{\partial \varepsilon_h} < 0$. This effect is used in immersion spectroscopy.

- *Bruggeman EMA* (effective medium approximation): We can model a molecular mixture where no host/guest functions may be attributed to any of the mixing partners.

$$\varepsilon = \varepsilon_h \quad \Rightarrow \quad 0 = \sum_j p_j \frac{\varepsilon_j - \varepsilon}{\varepsilon_j + 2\varepsilon}. \tag{3.29}$$

4 Interfaces - Fresnel equations

4.1 Motivation and first considerations

We want to model a system of two media with a plane, flat surface and want to describe the reflectivity and transmittance. We can calculate the reflected and transmitted fields using

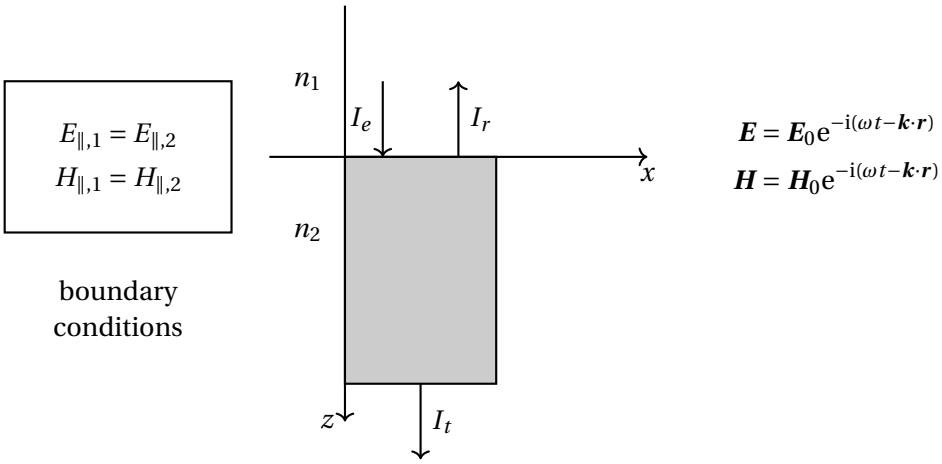

Figure 9: Model of our system: For $z < 0$ we have medium one n_1 and for $z > 0$ we have medium two n_2 with a plane, flat surface.

MAXWELL's boundary conditions of the parallel component of electric and magnetic field (c. f. figure 9). Assuming a non-magnetic medium we can express FARADAY's law as

$$\vec{\nabla} \times \boldsymbol{E} = -\frac{\partial \boldsymbol{B}}{\partial t} = -\mu_0 \frac{\partial H}{\partial t} = \mathrm{i}\omega\mu_0 \boldsymbol{H}. \tag{4.1}$$

Furthermore we can write $\vec{\nabla} \times \boldsymbol{E}$ as

$$\vec{\nabla} \times \boldsymbol{E} = \begin{vmatrix} \hat{\mathbf{e}}_x & \hat{\mathbf{e}}_y & \hat{\mathbf{e}}_z \\ \partial x & \partial y & \partial z \\ E_x & E_y & E_z \end{vmatrix} = \mathrm{i} \begin{vmatrix} \hat{\mathbf{e}}_x & \hat{\mathbf{e}}_y & \hat{\mathbf{e}}_z \\ k_x & k_y & k_z \\ E_x & E_y & E_z \end{vmatrix} = \mathrm{i}\boldsymbol{k} \times \boldsymbol{E}$$

$$\Rightarrow \omega\mu_0 \boldsymbol{H} = \boldsymbol{k} \times \boldsymbol{E} \quad \text{with} \quad \boldsymbol{k} = \frac{\omega}{c} n \hat{\mathbf{e}} \quad , \quad \hat{\mathbf{e}} \text{ propagation vector.} \tag{4.2}$$

Finally we find the following relation connecting magnetic and electric field

$$\boldsymbol{H} = \frac{n}{\mu_0 c} \boldsymbol{e} \times \boldsymbol{E}. \tag{4.3}$$

4.2 Special case - normal incidence

First we only want to consider the case of normal incidence onto the interface. Without loss of generality the electric field is then considered to only have a x-component.

We can now write the magnetic field $\boldsymbol{H}$ as

$$\boldsymbol{H} = \frac{n}{\mu_0 c}\begin{vmatrix} \hat{\mathbf{e}}_x & \hat{\mathbf{e}}_y & \hat{\mathbf{e}}_z \\ 0 & 0 & \pm 1 \\ \mathrm{E} & 0 & 0 \end{vmatrix}. \tag{4.4}$$

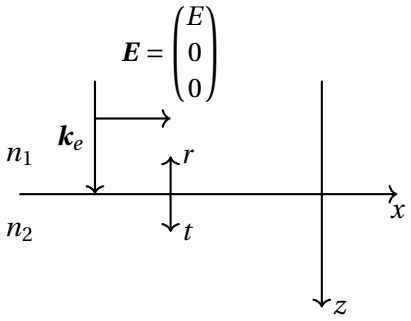

Figure 10: Schematics of the problem of normal incidence.

For the three different components we then obtain

$$\boldsymbol{H}_e = \frac{n_1}{\mu_0 c} E_e \hat{\mathbf{e}}_y, \quad \boldsymbol{H}_t = \frac{n_2}{\mu_0 c} E_t \hat{\mathbf{e}}_y, \quad \boldsymbol{H}_r = -\frac{n_1}{\mu_0 c} E_r \hat{\mathbf{e}}_y.$$

Now we demand the continuity of the normal components of the electric field

$$E_{\parallel,1} = E_{\parallel,2} \Rightarrow E_e + E_r = E_t \quad \text{with} \quad t \equiv \frac{E_t}{E_e}, r \equiv \frac{E_r}{E_e} \quad \Rightarrow \quad 1 + r = t \tag{4.5}$$

$$\begin{aligned} H_{\parallel,1} = H_{\parallel,2} &\Rightarrow n_1 E_e - n_1 E_r = n_2 E_t \\ &\Rightarrow n_1 - n_1 r = n_2 t \overset{(4.5)}{=} n_2(1+r) \\ &\Rightarrow n_1 - n_2 = r(n_1 + n_2). \end{aligned} \tag{4.6}$$

Now combining (4.5) and (4.6) we find FRESNEL's equations of normal incidence.

Fresnel equations for normal incidence

$$r = \frac{n_1 - n_2}{n_1 + n_2} \quad \text{and} \quad t = \frac{2n_1}{n_1 + n_2}. \tag{4.7}$$

We want to add some remarks to these equations. First, we note that the intensity I is proportional to the square of the modulus of the electric field giving us a reflectivity of

$$R = |r|^2 = \left|\frac{n_1 - \hat{n}_2}{n_1 + \hat{n}_2}\right|^2 \quad \text{for glass} \quad (n_1 = 1, n_2 = 1.5) \quad R = \left|\frac{1 - 1.5}{1 + 1.5}\right|^2 = 4\,\%. \tag{4.8}$$

Note that the refractive index may be complex. For example, let us consider a boundary between air and a metal $n_2 = n + \mathrm{i}k$ with $n \ll k$. Then we have

$$R = \left|\frac{1 - (n + \mathrm{i}k)}{1 + (n + \mathrm{i}k)}\right|^2 = \left.\frac{(1-n)^2 + k^2}{(1+n)^2 + k^2}\right|_{n \to 0} = 1 = 100\,\%. \tag{4.9}$$

This is the classical metallic reflection.
For low frequencies $\omega \to 0$ we can model the reflection on a metal by the HAGEN-RUBENS formula

$$R\Big|_{\omega \to 0} \approx 1 - \sqrt{\frac{8\varepsilon_0 \omega}{\sigma_{\mathrm{stat}}}}, \tag{4.10}$$

where σ_{stat} is the static conductivity. Furthermore we note that since $r = |r|\mathrm{e}^{\mathrm{i}\varphi}$ we have a phase shift if $n_1 < n_2$

$$n_1 < n_2 \quad \Rightarrow \quad r < 0, \phi = \pi. \tag{4.11}$$

We also notice that t and r may be complex, while T and R are real with $T + R \leq 1$.

4.3 Oblique incidence

4.3.1 Fresnel formulas

We now want to generalize formula (4.7) for oblique angle angles on the surface. We assume that the plane of incidence is the xz-plane. For this scenario we have to consider two different cases:

- s-polarization: $\boldsymbol{E} \perp$ incidence plane
  $\boldsymbol{E}_s = \begin{pmatrix} 0 \\ E \\ 0 \end{pmatrix}, \boldsymbol{H}_s = \begin{pmatrix} H_x \\ 0 \\ H_y \end{pmatrix}$ TE-wave
- p-polarization: $\boldsymbol{E} \parallel$ incidence plane
  $\boldsymbol{E}_s = \begin{pmatrix} E_x \\ 0 \\ E_z \end{pmatrix}, \boldsymbol{H}_s = \begin{pmatrix} 0 \\ H \\ 0 \end{pmatrix}$ TM-wave

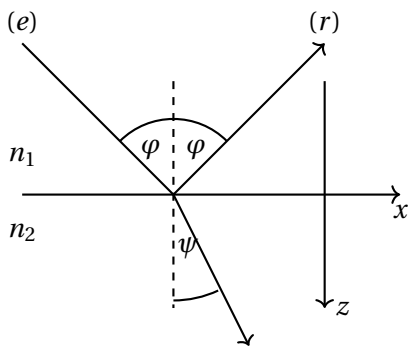

Figure 11: Geometry for oblique incidence.

We want to perform the following derivations for s-polarization. Using the boundary conditions $E_{\parallel,1} = E_{\parallel,2}$ we find $E_e + E_r = E_t$ and subsequently $1 + r = t$ analogous to (4.5). The boundary conditions for H lead to

$$H_{\parallel,1} = H_{\parallel,2} \quad \Rightarrow \quad H_{e,x} + H_{r,x} = H_{t,x}. \tag{4.12}$$

The unit propagation vectors can be read from figure 11

$$\hat{\mathbf{e}}_e = \begin{pmatrix} \sin\varphi \\ 0 \\ \cos\varphi \end{pmatrix}, \quad \hat{\mathbf{e}}_r \begin{pmatrix} \sin\varphi \\ 0 \\ -\cos\varphi \end{pmatrix}, \quad \hat{\mathbf{e}}_t = \begin{pmatrix} \sin\psi \\ 0 \\ \cos\psi \end{pmatrix}. \tag{4.13}$$

Using equation (4.3) we can calculate the magnetic field as

$$\begin{aligned} \boldsymbol{H}_e &= \frac{n_1}{\mu_0 c}\hat{\mathbf{e}}_e \times \boldsymbol{E} = \frac{n_1}{\mu_0 c}\begin{vmatrix} \hat{\mathbf{e}}_x & \hat{\mathbf{e}}_y & \hat{\mathbf{e}}_z \\ \sin\varphi & 0 & \cos\varphi \\ 0 & E_e & 0 \end{vmatrix} = -\frac{n_1}{\mu_0 c}\cos\varphi E_e \hat{\mathbf{e}}_x + \ldots \\ \boldsymbol{H}_r &= +\frac{n_1}{\mu_0 c}\cos\varphi E_r \hat{\mathbf{e}}_x + \ldots \qquad \boldsymbol{H}_t = -\frac{n_2}{\mu_0 c}\cos\psi E_t \hat{\mathbf{e}}_x + \ldots. \end{aligned} \tag{4.14}$$

Now substituting (4.14) into (4.12) we find

$$\begin{aligned} & n_1\cos\varphi E_e - n_1\cos\varphi E_r = n_2\cos\psi E_t \\ \Rightarrow\ & n_1\cos\varphi - n_1\cos\varphi r = n_2\cos\psi t = n_2\cos\psi(1+r) \\ \Rightarrow\ & n_1\cos\varphi - n_2\cos\psi = (n_1\cos\varphi + n_2\cos\psi)r \\ \Leftrightarrow\ & 2n_1\cos\varphi = (n_1\cos\varphi + n_2\cos\psi)t. \end{aligned} \tag{4.15}$$

We can now solve the results for t and r to obtain FRESNEL's equations for s-polarization. We can analogously derive the equations for p-polarized light. This leads us to

Fresnel equations for oblique incidence

$$r_s = \frac{n_1\cos\varphi - n_2\cos\psi}{n_1\cos\varphi + n_2\cos\psi} \quad \text{and} \quad t_s = \frac{2n_1\cos\varphi}{n_1\cos\varphi + n_2\cos\psi}$$
$$r_p = \frac{n_2\cos\varphi - n_1\cos\psi}{n_2\cos\varphi + n_1\cos\psi} \quad \text{and} \quad t_p = \frac{2n_1\cos\varphi}{n_2\cos\varphi + n_1\cos\psi}. \tag{4.16}$$

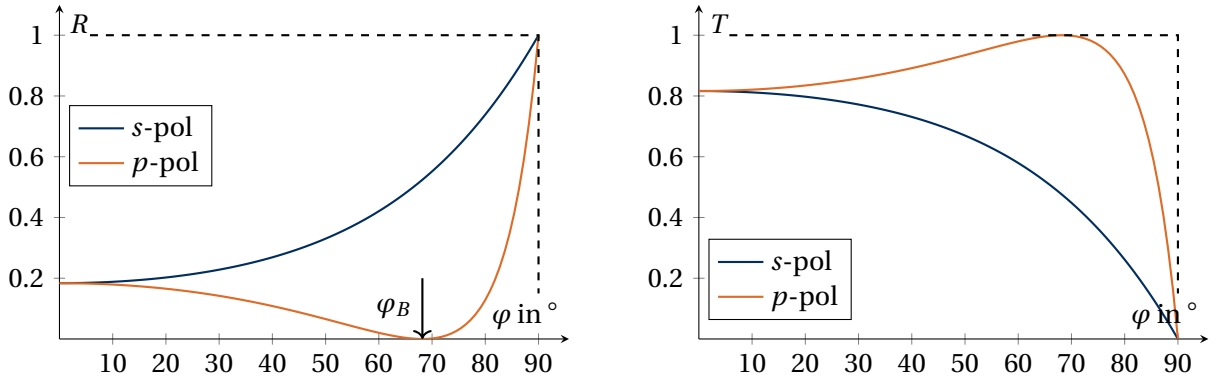

Figure 12: Transmission $T = 1 - R$ and reflection $R = |r|^2$ for two media with $n_1 = 1$ and $n_2 = 2.5$ for p- and s-polarization. For the calculation one can simply use equations (4.16) and substitute $\cos\psi = \sqrt{1 - (\frac{n_1}{n_2}\sin\varphi)^2}$ using SNELL's law.

The angle ϕ_B in figure 12 is called the *Brewster angle*, a point of zero reflection. This angle exists only for p-polarized light when the refracted and transmitted ray form a right angle $\varphi + \psi = \frac{\pi}{2}$. One can calculate the Brewster angle via

$$\tan\varphi_B = \frac{n_2}{n_1}. \tag{4.17}$$

4.3.2 Total internal reflection of light

For $n_1 > n_2$ we can determine the angle of total reflection as follows:

$$n_1\sin\varphi = n_2\underbrace{\sin\psi}_{=1} \quad \Rightarrow \sin\varphi_c = \frac{n_2}{n_1}. \tag{4.18}$$

Now we ask what happens if $\varphi > \varphi_c$. According to SNELL's law we would have $\sin\psi > 1$ and subsequently using $\sin^2\psi + \cos^2\psi = 1$ we would find $\cos^2\psi < 0$. This means that $\cos\psi$ must be purely imaginary. Thus we can express the reflection coefficient as

$$r_p = \frac{n_2\cos\varphi - n_1\cos\psi}{n_2\cos\varphi + n_1\cos\psi} = \sqrt{\frac{(n_2\cos\varphi)^2 + (n_1\cos\psi)^2}{(n_2\cos\varphi)^2 + (n_1\cos\psi)^2}}\mathrm{e}^{\mathrm{i}\delta_p} = |r_p|\mathrm{e}^{i\delta_p} \Rightarrow |r_p|^2 = 1. \tag{4.19}$$

We can see that $T = 1 - R = 0$, however, we find $t_p \neq 0$. This implies that the relation between t and T is not just the absolute square.

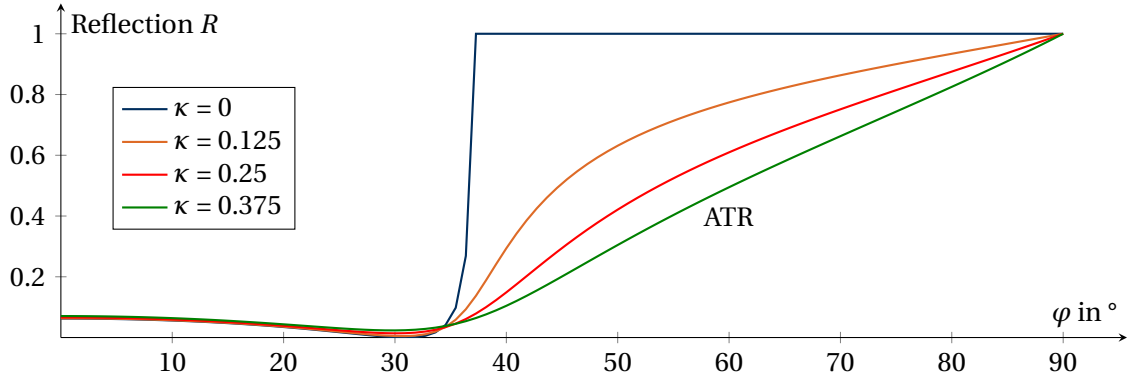

Figure 13: Total reflection for $n_1 > n_2$ with $n_1 = 2.5$ and $n_2 = 1.5 + \mathrm{i}\kappa$ where we plot the reflection for different values of absorption. We observe that the Brewster-effect reduces to a minimum we call a *Pseudo Brewster angle*. The effect of diminished reflection above the critical angle of total reflection is called attenuated total reflection (ATR).

Let us now consider the transmitted wave for assumed perfect total reflection. We can write $\boldsymbol{k}_t$ as

$$\boldsymbol{k}_t = \frac{\omega}{c} n_2 \, \hat{\mathbf{e}}_t = \frac{\omega}{c} n_2 \sin\psi \, \hat{\mathbf{e}}_x + \frac{\omega}{c} n_2 \cos\psi \, \hat{\mathbf{e}}_z. \tag{4.20}$$

For perfect total reflection $\cos\psi$ is completely imaginary $\cos\psi = \mathrm{i}|\cos\psi|$. Then the transmitted phase of the field is

$$\mathrm{e}^{-\mathrm{i}(\omega t - \boldsymbol{k}_t \cdot \boldsymbol{r})} = \mathrm{e}^{-\mathrm{i}(\omega t - \frac{\omega}{c} n_2 \sin\psi x)} \cdot \mathrm{e}^{-\frac{\omega}{c} n_2 |\cos\psi| z}. \tag{4.21}$$

The last part describes a dampening of the field in the medium. This evanescent wave has a penetration depth of

$$l_{\mathrm{pen}} = \frac{c}{\omega n_2 |\cos\psi|} \propto \lambda. \tag{4.22}$$

This means the electric field of the transmitted wave traveling in x-direction penetrates into the material leading to a nonzero transmission coefficient, while the total transmittance T is zero. For a complex refractive index $\hat{n}_2$ we will have absorption $A \neq 0$ leading to attenuated total reflection ATR at the Brewster angle.

4.3.3 Intensity coefficients

We want to discuss the intensity coefficients R and T for different cases. The intensity of the light is proportional to the average of the propagation velocity v times the energy density w

$$I \propto \langle v \cdot w \rangle \propto \left\langle \frac{c}{n} n^2 |E|^2 \right\rangle = n|E|^2. \tag{4.23}$$

Let us start with the first case of normal incidence (n. i.) and real refractive indices. Then we find

$$R = \left(\frac{n_1 - n_2}{n_1 + n_2} \right)^2, \quad T = \frac{n_2}{n_1} \left| \frac{2n_1}{n_1 + n_2} \right|^2 = \frac{4 n_1 n_2}{(n_1 + n_2)^2} \quad \text{with} \quad T + R = 1. \tag{4.24}$$

In the case of oblique incidence, however, the velocity of reflected and transmitted wave is given geometrically by $v_{r,z} = v_t \cos\varphi$ and $v_{t,z} = v_r \cos\psi$. The the reflected and transmitted intensities are

$$T = \frac{n_2 \cos\psi}{n_1 \cos\varphi}|t|^2, \quad \text{and} \quad R = \frac{n_1 \cos\varphi}{n_2 \cos\varphi}|r|^2 = |r|^2. \tag{4.25}$$

For oblique incidence with complex refractive index $\hat{n}_2$ the transmitted wave is given by

$$\begin{aligned} E &= E_0 \mathrm{e}^{-\mathrm{i}(\omega t - \boldsymbol{k_z}\cdot\boldsymbol{r})} = E_0 \mathrm{e}^{-\mathrm{i}(\omega t - k_x x - k_z z)} \\ \text{with} \quad k_x &= \frac{\omega}{c} \underbrace{\hat{n}_2 \sin\psi}_{n_1 \sin\varphi} = \text{ real} \\ k_z &= \frac{\omega}{c}\hat{n}_2 \cos\psi = \mathrm{Re}\, k_z + \mathrm{i}\,\mathrm{Im}\, k_z \\ \Rightarrow E &= E_0 \mathrm{e}^{-\mathrm{Im}\, k_z z} \mathrm{e}^{-\mathrm{i}(\omega t - k_x x - \mathrm{Re}(k_z) z)}. \end{aligned} \tag{4.26}$$

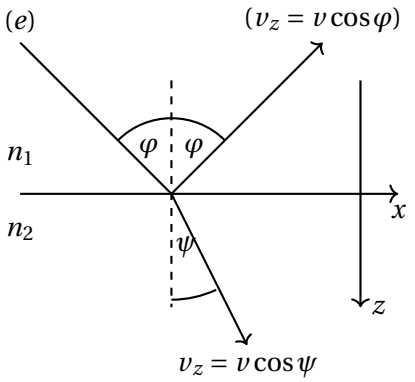

Figure 14: The intensity is only determined by the z-component of the velocity vector.

The reflection and transmission intensities can then be generalized to

Transmission and reflectance

$$R = |r|^2 \quad \text{and} \quad T = \frac{\mathrm{Re}(\hat{n}_2 \cos\psi)}{n_1 \cos\varphi}|t|^2. \tag{4.27}$$

Example: Metallic surface

We want to discuss the example of a metal surface where $\hat{n}_2 = n - \mathrm{i}\kappa$. Then we have for transmission and reflectance

$$\begin{aligned} R &= \left|\frac{1-\hat{n}_2}{1+\hat{n}_2}\right|^2 = \left|\frac{1-n-\mathrm{i}k}{1-n+\mathrm{i}k}\right|^2 = \frac{(1-n)^2+k^2}{(1+n)^2+k^2} \\ T &= n\left|\frac{2}{1+n+\mathrm{i}k}\right|^2 = \frac{4n}{(1+n)^2+k^2}. \end{aligned} \tag{4.28}$$

5 Multiple internal reflections in layered systems

5.1 Incoherent case (slab of material)

5.1.1 No absorption

First we want to consider the case of a non-absorbing slab of material as shown in figure 15. The total transmission of the slab can be calculated by considering all possible paths a light ray can take to arrive on the other side of the thick slab

$$\begin{aligned} T &= T_{12}T_{21} + T_{12}R_{21}^2T_{21} + T_{12}R_{21}^4T_{21} + \dots \\ &= T_{12}T_{21}\sum_{n=0}^{\infty} R_{21}^{(2n)} = \frac{T_{12}T_{21}}{1-R_{21}^2}. \end{aligned} \tag{5.1}$$

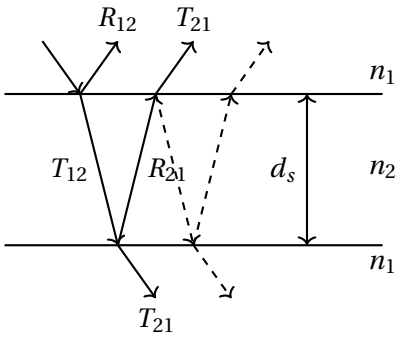

Figure 15: Non-absorbing slab.

For the special case of $T_{12} = T_{21} = 1 - R_{21}$ we arrive at

$$T = \frac{(1-R_{21})^2}{(1-R_{21})(1+R_{21})} = \frac{1-R_{21}}{1+R_{21}} \quad \text{and} \quad R = \frac{2R_{21}}{1+R_{21}}. \tag{5.2}$$

Using FRESNEL's formulas for normal incidence we find for $n_1 = 1, n_2 = n$

$$R_{21} = \left(\frac{n_1-n_2}{n_1+n_2}\right)^2 = \frac{(1-n)^2}{(1+n)^2} \quad \Rightarrow \quad T = \frac{2n}{1+n^2}. \tag{5.3}$$

5.1.2 Absorbing slab

Before we consider absorption we want to right down the transmission of the slab for oblique incidence

$$\begin{aligned} T &= \frac{T_{12}T_{21}}{1-R_{21}^2} \quad \text{non-abs.} \quad T_{12} = \frac{n_2\cos\psi}{n_1\cos\varphi}|t_{12}|^2, \quad T_{21} = \frac{n_1\cos\varphi}{n_2\cos\psi}|t_{21}|^2 \\ &= \frac{|t_{12}|^2|t_{21}|^2}{1-|r_{21}|^4}. \end{aligned} \tag{5.4}$$

Wir absorption we have to consider the dampening of the electromagnetic field

$$\begin{aligned} \boldsymbol{E} &= \boldsymbol{E}_0 \mathrm{e}^{-\mathrm{i}(\omega t - \boldsymbol{k}\cdot\boldsymbol{r})}, \quad \text{with} \quad \boldsymbol{k}\cdot\boldsymbol{r} = \frac{\omega}{c}(\hat{n}_2\sin\psi x + \hat{n}_2\cos\psi z) \\ &= \boldsymbol{E}_0 \exp\Big(-\mathrm{i}(\omega t - \frac{\omega}{c}n_1\sin\varphi x)\Big)\exp\Big(\mathrm{i}\frac{\omega}{c}\hat{n}_2\cos\psi z\Big) \\ \Rightarrow |E|^2 &= |E_0|^2 \underbrace{\exp\Big(-2\frac{\omega}{c}\operatorname{Im}(\hat{n}_2\cos\psi)z\Big)}_{\text{damping factor}}. \end{aligned} \tag{5.5}$$

Furthermore, if we express $\hat{n}_2 \cos\psi$ in terms of the angle of the incidence ray

$$\hat{n}_2 \cos\psi = \sqrt{\hat{n}_2^2 - n_1^2 \sin^2\varphi} \tag{5.6}$$

we finally arrive at

Transmission and reflection of a thick slab

$$T = \frac{|t_{12}|^2 |t_{21}|^2 \exp\left(-\frac{2\omega}{c} d_s \operatorname{Im}\sqrt{\hat{n}_2^2 - n_1^2 \sin^2\varphi}\right)}{1 - |r_{21}|^4 \exp\left(-\frac{4\omega}{c} d_s \operatorname{Im}\sqrt{\hat{n}_2^2 - n_1^2 \sin^2\varphi}\right)} \tag{5.7}$$

$$R = |r_{12}|^2 + \frac{|t_{12}|^2 |t_{21}|^2 |r_{21}|^2 \exp\left(-\frac{4\omega}{c} d_s \operatorname{Im}\sqrt{\hat{n}_2^2 - n_1^2 \sin^2\varphi}\right)}{1 - |r_{21}|^4 \exp\left(-\frac{4\omega}{c} d_s \operatorname{Im}\sqrt{\hat{n}_2^2 - n_1^2 \sin^2\varphi}\right)} \tag{5.8}$$

We note that for an infinitely thick slab $d_s \to \infty$ we obtain $T \to 0$ and $R \to |r_{12}|^2$ as expected.

5.2 Coherent case (thin layer)

We now want to consider the case of a thin layer with $d \ll l_{\text{coh}}$. Analogously to the incoherent case we can express the transmission coefficients (since now we have to consider interference) through the layer as a geometric series which leads us to

$$\begin{aligned} t_{123} &= t_{12} e^{i\delta} t_{23} + t_{12} e^{i\delta} r_{23} e^{i\delta} r_{21} e^{i\delta} t_{23} + \dots \\ &= t_{12} t_{23} e^{i\delta} \sum_{n=0}^{\infty} (r_{23} r_{21} e^{2i\delta})^n \\ &= \frac{t_{12} t_{23} e^{i\delta}}{1 - r_{21} r_{23} e^{2i\delta}} = \frac{t_{12} t_{23} e^{i\delta}}{1 + r_{12} r_{23} e^{2i\delta}} \end{aligned} \tag{5.9}$$

$$r_{123} = \frac{r_{12} + r_{23} e^{2i\delta}}{1 + r_{12} r_{23} e^{2i\delta}}. \tag{5.10}$$

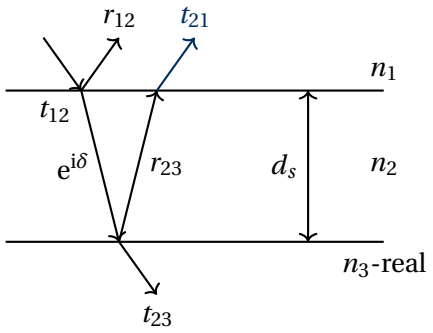

Figure 16: Thin, non-absorbing layer.

5.2.1 Normal incidence

Let us further discuss the special case of normal incidence. Here we can express the phase δ simply as

$$\delta = kd = \frac{\omega}{c} \hat{n}_2 d = \frac{2\pi}{\lambda} \hat{n}_2 d = 2\pi\nu\hat{n}_2 d. \tag{5.11}$$

Thus we collect a total phase of $2\delta = 4\pi\nu\hat{n}_2 d$ per loop in the thin layer. We now ask the question when the reflection of this slab goes to zero. One solution one can immediately verify is

$$r_{12} = r_{23} \quad \text{and} \quad e^{2i\delta} = -1 \quad \Rightarrow \quad 2\delta = \pi = 4\pi\nu\hat{n}_2 d \Rightarrow \hat{n}_2 d = \frac{\lambda}{4}. \tag{5.12}$$

This means the optical thickness of the medium corresponds to a quarter wave (QW) plate. For the design of a QW layer we need to establish $r_{12} = r_{23}$

$$\begin{aligned} r_{12} = r_{23}\Big|_{\text{n. i.}} \quad & \frac{n_1 - n_2}{n_1 + n_2} = \frac{n_2 - n_3}{n_2 + n_3} \\ \Rightarrow (n_1 - n_2)(n_2 + n_3) &= (n_2 - n_3)(n_1 + n_2) \\ \Rightarrow n_2^2 = n_1 n_3 \Rightarrow n_2 = \sqrt{n_1 n_3} \quad &\text{and} \quad n_2 d = \frac{\lambda}{4}. \end{aligned} \tag{5.13}$$

We deduce that for $n_1 = 1$ we can only achieve anti-reflection with a single coating if $n_2 < n_3 = n_{\text{sub}}$. Since the refractive index of the layer is lower than of the substrate we call this a *low index coating* or a *single layer anti reflection coating* (SLAR). We also want to visualize the effect of anti-reflection with a single layer. This is shown in figure 17. Because $r_{23} = -|r_{23}|$ we observe a phase shift of π at the reflection on the back of the layer. The reflected wave is then phase shifted by π which leads to destructive interference of the front and back reflection of the thin film.

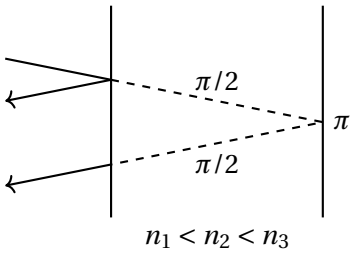

Figure 17: Single layer low index AR coating.

If, however, we instead choose a *high index* coating we will not have a phase shift on the back of the thin film layer as displayed in figure 18. This will lead to constructive interference of the front and backside reflection of the thin film. The resulting reflectivity then matches the reflectivity of the bare substrate without any coating.

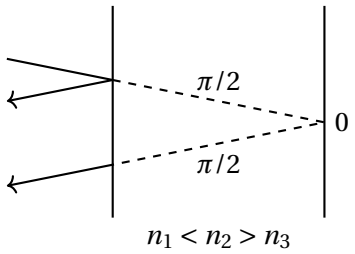

Figure 18: Single layer high index coating.

5.2.2 Basic QW applications

Instead of a SLAR coating we can also try to create a stack of dielectric QW layers with alternating high and low refractive index. We demand that the optical path is constant in both layers

$$n_L d_L = n_H d_H = \frac{\lambda}{4}. \tag{5.14}$$

Such a scheme of a QW stack is displayed in figure 19. If the number of periods goes to infinity we will reach a theoretical reflectivity of $R = 1$ at λ_0. We might also want to raise the question, at which wavelength range we will have high reflectivity. This is called the *rejection band*. The width of the rejection band is generally a function of

$$w_{\text{rejec. band}} = f\left(\frac{n_H - n_L}{n_H + n_L}\right). \tag{5.15}$$

For a broadband high reflector we need to maximize the ratio of high and low refractive index of the layers.

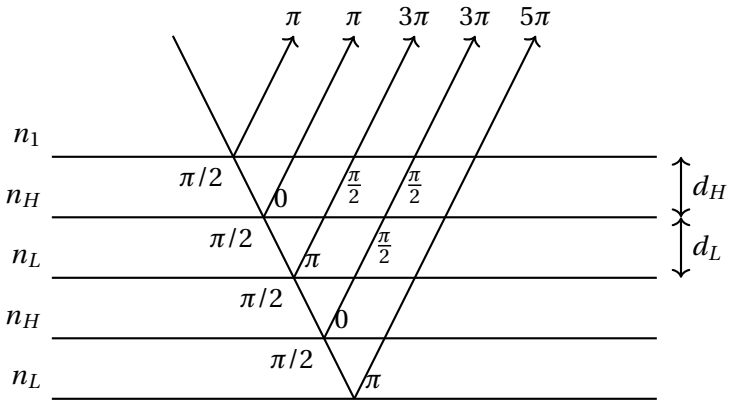

Figure 19: Scheme of a high reflection QW stack.

Furthermore we can use a QW stack to create frequency filters. For that we take a look at figure 20 (left). The figure shows the rejection band of a QW stack. Only at the center frequency $1/\lambda_0$ we have perfect reflectivity. At the edges of the rejection band one can construct long/short pass frequency filters. For the modeling of thinfilm stacks one can use the following notation:

$$\text{air}|\text{HLHLHLH}|\text{sub} = \text{air}|(\text{HL})^N\text{H}|\text{sub}, \tag{5.16}$$

where N is the number of alternating layers. For even N we can also write this as

$$\text{air}|(\text{HL})^{N/2}\text{H}(\text{LH})^{N/2}|\text{sub}. \tag{5.17}$$

We can also design a narrow bandpass filter using QW stacks. For that we model a new stack

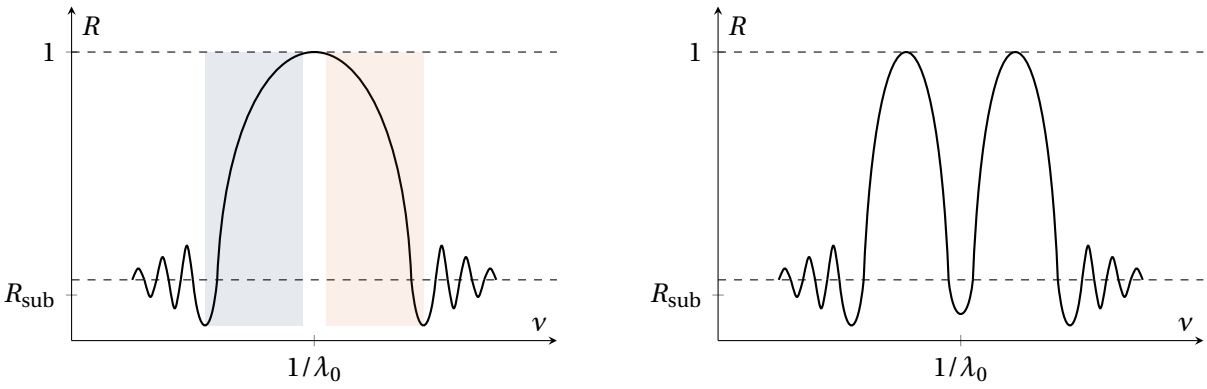

Figure 20: Left: Rejection band of a QW stack. In blue we see a spectral region for a possible *long pass edge filter* and in orange a region for a *short pass edge filter*.
Right: With an additional high index layer in the middle of the QW stack one can achieve a narrow bandpass filter.

with an additional high index layer in the middle of the stack. Since HH-layers or LL-layers do not contribute for reflection (c. f. HW layers), we can simplify the effect of the QW stack

to

$$\begin{aligned}\text{air}|(\text{HL})^{N/2}\text{HH}(\text{LH})^{N/2}|\text{sub} &= \text{air}|(\text{HL})^{\frac{N}{2}-1}\text{HLLH}(\text{LH})^{\frac{N}{2}-1}|\text{sub} \\ &= \text{air}|(\text{HL})^{\frac{N}{2}-1}\text{HH}(\text{LH})^{\frac{N}{2}-1}|\text{sub} = \ldots \\ &= \text{air}|\text{sub} \quad \text{at } \lambda_0. \end{aligned} \tag{5.18}$$

The resulting rejection band of such a layer is shown in figure 20 (right).

5.2.3 Half wave layers (HW)

We now want to consider half wave layers. For that we have $\delta = \pi \Rightarrow e^{2i\delta} = 1$ and thus equations (5.9) and (5.10) become

$$r_{123} = \frac{r_{12} + r_{23}}{1 + r_{12} r_{23}}, \quad t_{123} = -\frac{t_{12} t_{23}}{1 + r_{12} r_{23}} \quad \text{with} \quad n_2 d = \frac{1}{2\nu} = \frac{\lambda}{2}. \tag{5.19}$$

Let us inspect first the trivial case $\delta = 0$ resulting in $d = 0$ and $n_3 = n_1$. Then we have

$$r_{123}\Big|_{d=0} = \frac{r_{12} + r_{21}}{1 + r_{12} r_{21}} = 0 \quad \text{because} \quad r_{12} = \frac{n_1 - n_2}{n_1 + n_2} = -r_{21}. \tag{5.20}$$

This is consistent expectation for a layer thickness of zero where we would have no interface. Now we move on to the HW layer. We can write the transmission coefficient as

$$\begin{aligned} t_{123} &= -\frac{t_{12} t_{23}}{1 + r_{12} r_{23}} = -\frac{4 n_1 n_2}{(n_1 + n_2)(n_2 + n_3) + (n_1 - n_2)(n_2 - n_3)} \quad \text{where} \quad t_{ij} = \frac{2 n_i}{n_i + n_j} \\ &= -\frac{4 n_1 n_2}{2 n_1 n_2 + 2 n_2 n_3} = -\frac{2 n_1}{n_1 + n_3}. \end{aligned} \tag{5.21}$$

The transmission can now be calculated as

$$T_{123} = \frac{n_3}{n_1}\left|\frac{2 n_1}{n_1 + n_3}\right|^2 = \frac{4 n_1 n_2}{(n_1 + n_3)^2} = T_{13}. \tag{5.22}$$

We conclude that the transmittance does not depend on medium 2.

5.2.4 Single film spectrum

We now want to calculate the transmission of a single film as a function of frequency. We start with equation (5.9)

$$T = \frac{n_3}{n_1}|t_{123}|^2 = \frac{n_3}{n_1}\left|\frac{t_{12} t_{23} e^{i\delta}}{1 + r_{12} r_{23} e^{2i\delta}}\right|^2 = \frac{n_3}{n_1}\frac{t_{12}^2 t_{23}^2}{1 + r_{12}^2 r_{23}^2 + 2 r_1 r_2 \cos(2\delta)}. \tag{5.23}$$

If we assume low dispersion, the term $r_{12}r_{23}$ will be wakly dispersive and $\cos(2\delta)$ the dominating frequency dependence. This leads to a quasi-periodic behaviour of the transmittance $T(\nu)$. Let us now examine the extrema of $T(\nu)$. For $\delta = m\pi$ we find $n_2 d = m\frac{\lambda}{4}$:

$$\begin{aligned} m=1: &\quad n_2 d = \frac{\lambda}{4} \quad \text{QW layer} \\ m=2: &\quad n_2 d = \frac{\lambda}{2} \quad \text{HW layer} \quad R = R_{\text{sub}}, T = T_{\text{sub}} \\ m=3: &\quad n_2 d = \frac{3\lambda}{4} \quad \text{QW layer} \quad . \end{aligned} \tag{5.24}$$

We can generalize these findings to

$$m \quad \text{odd: QW-points} \qquad \text{and} \quad m \quad \text{even: HW-points} \tag{5.25}$$

$$\nu_m = \frac{m}{4n_2 d} \qquad \Delta\nu = \nu_{m+1} - \nu_m = \frac{1}{4n_2 d}. \tag{5.26}$$

The spectral behavior of high and low index layers is shown in figure 21. Notice that for a low refractive index layer we can achieve anti-reflection as already derived in section 5.2.1.

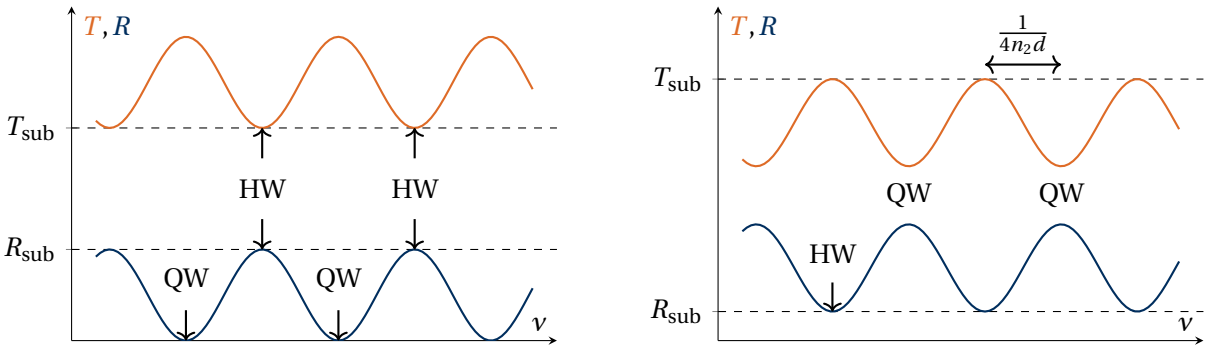

Figure 21: Left: Low refractive index coating. $n_1 < n_2 < n_3$, $R_{\text{QW}} < R_{\text{sub}}$.
Right: High refractive index coating. $n_2 > n_1, n_3$, $R_{\text{QW}} > R_{\text{sub}}$.

5.3 Possible complications

5.3.1 Oblique incidence

In the following we want to discuss several cases complicating the frequency behavior of a single film spectrum. If we consider oblique incidence angles we need to take different optical paths into account as shown in figure 22. We can actually show that the total phase difference can be simply calculated by using the z-component of the k-vector

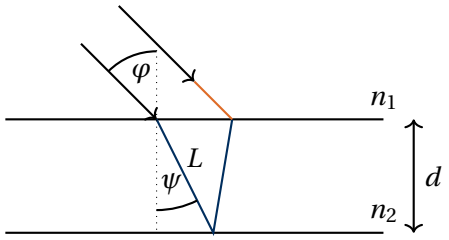

Figure 22: Optical path difference for oblique incidence.

$$\begin{aligned} 2\delta &= k_z \cdot 2d = \frac{4\pi}{\lambda} n_2 \cos\psi \\ &= 4\pi\nu d\sqrt{n_2^2 - n_1^2 \sin^2\varphi}, \end{aligned} \tag{5.27}$$

where we used SNELL's law of refraction to replace $\cos\psi$. We can verify this result by calculating the total phase difference geometrically using the lengths given in blue and orange in figure 22

$$\begin{aligned}
2\delta &= \frac{2\pi}{\lambda}\left[n_2\frac{2d}{\cos\psi} - n_1 L\sin\varphi\right] \quad \text{with} \quad L = 2d\tan\psi \\
&= \frac{4\pi d}{\lambda}\left[\frac{n_2}{\cos\psi} - \frac{n_1\sin\psi\sin\varphi}{\cos\psi}\right] \quad \text{with} \quad \sin\psi = \frac{n_1}{n_2}\sin\varphi \\
&= \frac{4\pi d}{\lambda}\left[\frac{n_2^2 - n_1^2\sin^2\varphi}{n_2\cos\psi}\right] \quad \text{with} \quad n_2\cos\psi = \sqrt{n_2^2 - n_1^2\sin^2\varphi} \\
&= \frac{4\pi d}{\lambda}\sqrt{n_2^2 - n_1^2\sin^2\varphi}.
\end{aligned} \tag{5.28}$$

We also observe that the phase gets smaller $\frac{\partial}{\partial\varphi}(\delta) < 0$ for increasing angle of incidence. We can now directly compare the extrema of the thinfilm spectrum

$$\text{n. i.} \quad \nu_m = \frac{m}{4n_2 d}, \qquad \varphi \neq 0 \quad \nu_m = \frac{m}{4d\sqrt{n_2^2 - n_1^2\sin^2\varphi}}. \tag{5.29}$$

We call the pheonomena *angular shift*. For a QW layer ($m = 1$) the layer thickness is

$$d = \frac{\lambda_{\text{o.i.}}}{4\sqrt{n_2^2 - n_1^2\sin^2\varphi}}. \tag{5.30}$$

Alternatively we can calculate the refractive index of the second medium for given values of λ at normal and oblique incidence

$$n_2 = \frac{\lambda_{\text{n.i.}}}{\lambda_{\text{o.i.}}}\sqrt{n_2^2 - n_1^2\sin^2\varphi}\,\Big|\,(\ldots)^2 \quad \Rightarrow n_2 = \frac{n_1\sin\varphi}{\sqrt{1 - \dfrac{\lambda_{\text{o.i.}}^2}{\lambda_{\text{n.i.}}^2}}}. \tag{5.31}$$

For two measurements at oblique incidence this generalizes to

$$n_2 = n_1\sqrt{\frac{\lambda_b^2\sin^2\varphi_a - \lambda_a^2\sin^2\varphi_b}{\lambda_b^2 - \lambda_a^2}}. \tag{5.32}$$

5.3.2 Light absorption

We now want to incorporate absorption into our equations. For complex refractive indices δ becomes a complex quantity

$$\mathrm{e}^{\mathrm{i}\delta} = \mathrm{e}^{-\operatorname{Im}\delta}\mathrm{e}^{-\mathrm{i}\operatorname{Re}\delta} \quad \text{with} \quad 2\operatorname{Im}\delta = 4\pi\nu d\operatorname{Im}\hat{n}_2 = \alpha d. \tag{5.33}$$

The transmittance of the single film layer then becomes

$$\begin{aligned}
T &= \frac{n_3\cos\varphi_3}{n_1\cos\varphi}|t_{123}|^2 \quad \text{with} \quad t_{123} = \frac{t_{12}t_{23}\mathrm{e}^{\mathrm{i}\delta}}{1 + r_{12}r_{23}\mathrm{e}^{2\mathrm{i}\delta}}, \\
&= \frac{n_3\cos\varphi_3}{n_1\cos\varphi}\frac{|t_{12}|^2|t_{23}|^2\mathrm{e}^{-2\operatorname{Im}\delta}}{|1 + r_{12}r_{23}\mathrm{e}^{2\mathrm{i}\delta}|^2} \overset{\text{n.i.}}{=} \frac{n_3}{n_1}\frac{|t_{12}|^2|t_{23}|^2\mathrm{e}^{-\alpha d}}{|1 + r_{12}r_{23}\mathrm{e}^{2\mathrm{i}\delta}|^2}
\end{aligned} \tag{5.34}$$

The effect of absorption on the transmittance and reflectivity is shown in figure 23. Usually the absorption takes place at the edge of the visible spectrum to the ultraviolett spectrum (c. f. figure 2).

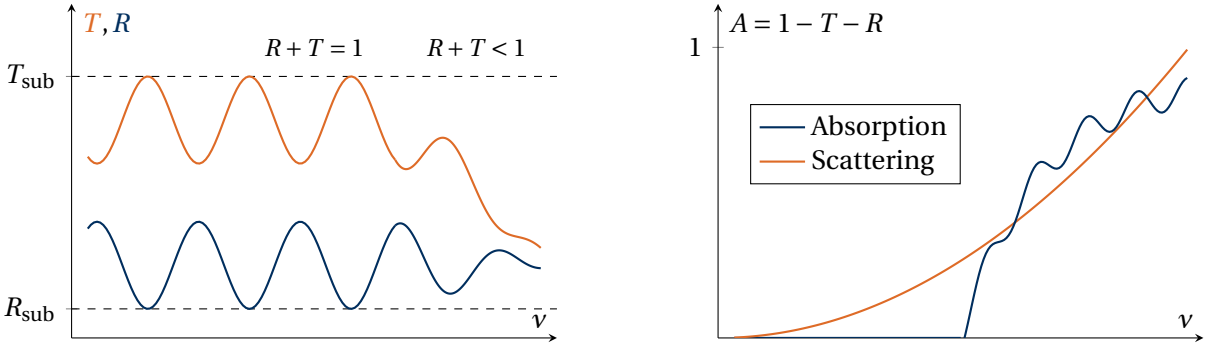

Figure 23: Light absorption (left) and scattering (only right) in a single film.

5.3.3 Rough surfaces

In the case of a large scale roughness where the periodicity of the rough surface Λ is larger than the wavelength λ we also observe scattering effects

$$S = \frac{I_s}{I_e} \quad \Rightarrow R + T + A + S = 1. \tag{5.35}$$

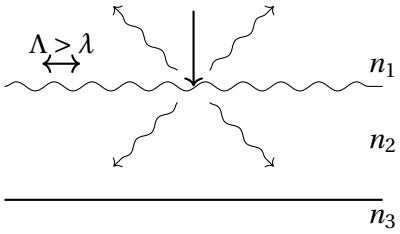

Figure 24: Scattering scheme.

In general scattering increases for lower wavelengths. If we only have T and R available for our thin film, it is often helpful to model the scattering $S(\nu)$ as a smooth function of $\propto \nu^2, \nu^4$, whereas absorption has a threshold character.

5.3.4 Gradient index coatings

In the following we want to consider weak refractive index gradients in single non-absorbing films. We can distinguish between two different types of coatings:

- Positive index gradient
- Negative index gradient.

The type of index gradient is defined as seen from the substrate, i. e. a film with increasing refractive index from the substrate towards the air is called a positive index gradient.

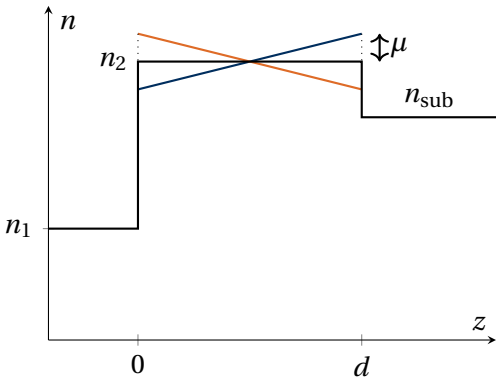

Figure 25: Refractive index gradient

We now want to discuss how the single film spectrum changes in the HW and QW points

$$\text{QW:}\quad r_{123} = \frac{r_{12} - r_{23}}{1 - r_{12} r_{23}}, \qquad \text{HW:}\quad r_{123} = \frac{r_{12} + r_{23}}{1 + r_{12} r_{23}}. \tag{5.36}$$

For simplicity we only consider the numerators of (5.36). Then we can make use of simple vector diagrams to determine the behavior of the single film at the QW points and HW points. This is displayed first without gradients in figure 26 and then including gradients in 27. As we can see, the reflectivity in the QW points is about the same for a gradient index layer, however, the reflectivity at the HW points changes. For a low index layer the reflectivity is above/below the reflectivity of the substrate for a positive/negative refractive index gradient. We can also visualize this in figure 28.

Schröders approximation

We now want to calculate the reflectivity for a gradient index layer with a weak refractive index gradient. We model the refractive index gradient as a linear function with a deviation μ from the mean index $\langle n \rangle$ (c. f. figure 25). At $z = 0$ we have $n = \langle n \rangle - \mu$ and at $z = d$ we have $n = \langle n \rangle + \mu$. A value $\mu > 0$ corresponds to a negative gradient, whereas $\mu < 0$ is a positive gradient. The coefficients of reflections are

$$r_{12} = \frac{1 - \langle n \rangle + \mu}{1 + \langle n \rangle - \mu} \quad \text{and} \quad r_{23} = \frac{\langle n \rangle + \mu - n_{\text{sub}}}{\langle n \rangle + \mu + n_{\text{sub}}} \quad \text{with} \quad r_{123} = \frac{r_{12} + r_{23} \mathrm{e}^{2\mathrm{i}\delta}}{1 + r_{12} r_{23} \mathrm{e}^{2\mathrm{i}\delta}}. \tag{5.37}$$

We now introduce SCHRÖDERS approximation as

$$\delta = 2\pi\nu \int_0^z n(z)\,\mathrm{d}z = 2\pi\nu \langle n \rangle d. \tag{5.38}$$

For a linear refractive index gradient this is equation is actually no approximation. First we consider the reflectivity at the HW points

$$\begin{aligned}
r_{123,\text{HW}} = \frac{r_{12} + r_{23}}{1 + r_{12} r_{23}} &= \frac{(1 - \langle n \rangle + \mu)(\langle n \rangle + \mu + n_{\text{sub}}) + (1 + \langle n \rangle - \mu)(\langle n \rangle + \mu - n_{\text{sub}})}{(1 + \langle n \rangle - \mu)(\langle n \rangle + \mu + n_{\text{sub}}) + (1 - \langle n \rangle + \mu)(\langle n \rangle + \mu - n_{\text{sub}})} \\
&\quad \text{terms} \quad \mu^2, \mu \langle n \rangle, \langle n \rangle^2, n_{\text{sub}} \quad \text{cancel out} \\
&= \frac{\langle n \rangle + \mu - \langle n \rangle n_{\text{sub}} + \mu n_{\text{sub}}}{\langle n \rangle + \mu + \langle n \rangle n_{\text{sub}} - \mu n_{\text{sub}}} \\
&= \frac{\langle n \rangle (1 - n_{\text{sub}}) + \mu(1 + n_{\text{sub}})}{\langle n \rangle (1 + n_{\text{sub}}) + \mu(1 - n_{\text{sub}})} = \frac{\langle n \rangle \dfrac{1 - n_{\text{sub}}}{1 + n_{\text{sub}}} + \mu}{\langle n \rangle + \mu \dfrac{1 - n_{\text{sub}}}{1 + n_{\text{sub}}}} \\
&= \frac{\langle n \rangle r_{13} + \mu}{\langle n \rangle + \mu r_{13}} = \frac{r_{13} + \dfrac{\mu}{\langle n \rangle}}{1 + r_{13} \dfrac{\mu}{\langle n \rangle}}.
\end{aligned} \tag{5.39}$$

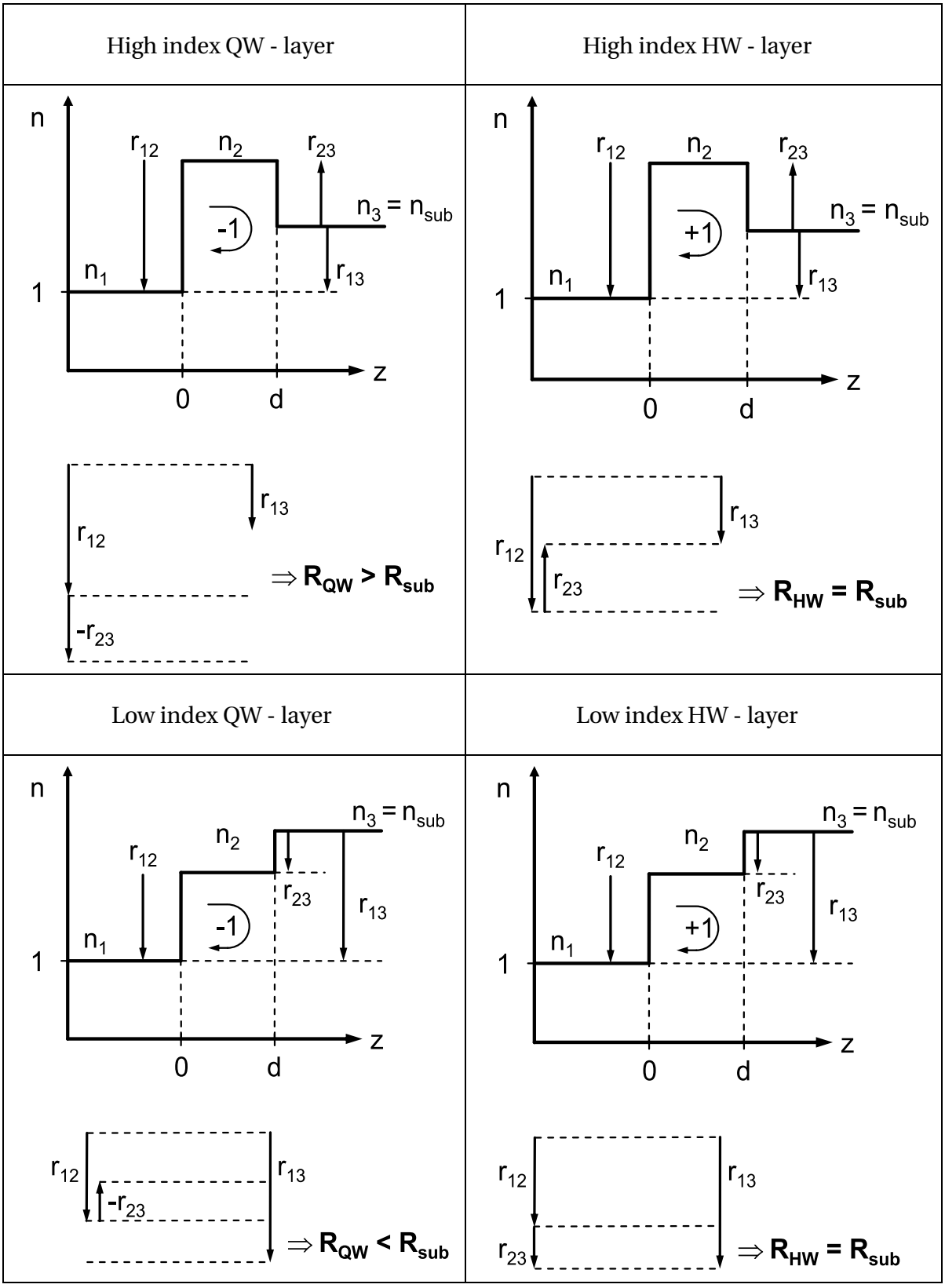

Figure 26: Illustration of the effect of QW and HW layers on the reflectance of an optical surface. Note that the vector diagrams are just qualitative pictures, since we neglect the denominator of the reflectivity of the single film. However, the qualitative results are correct.

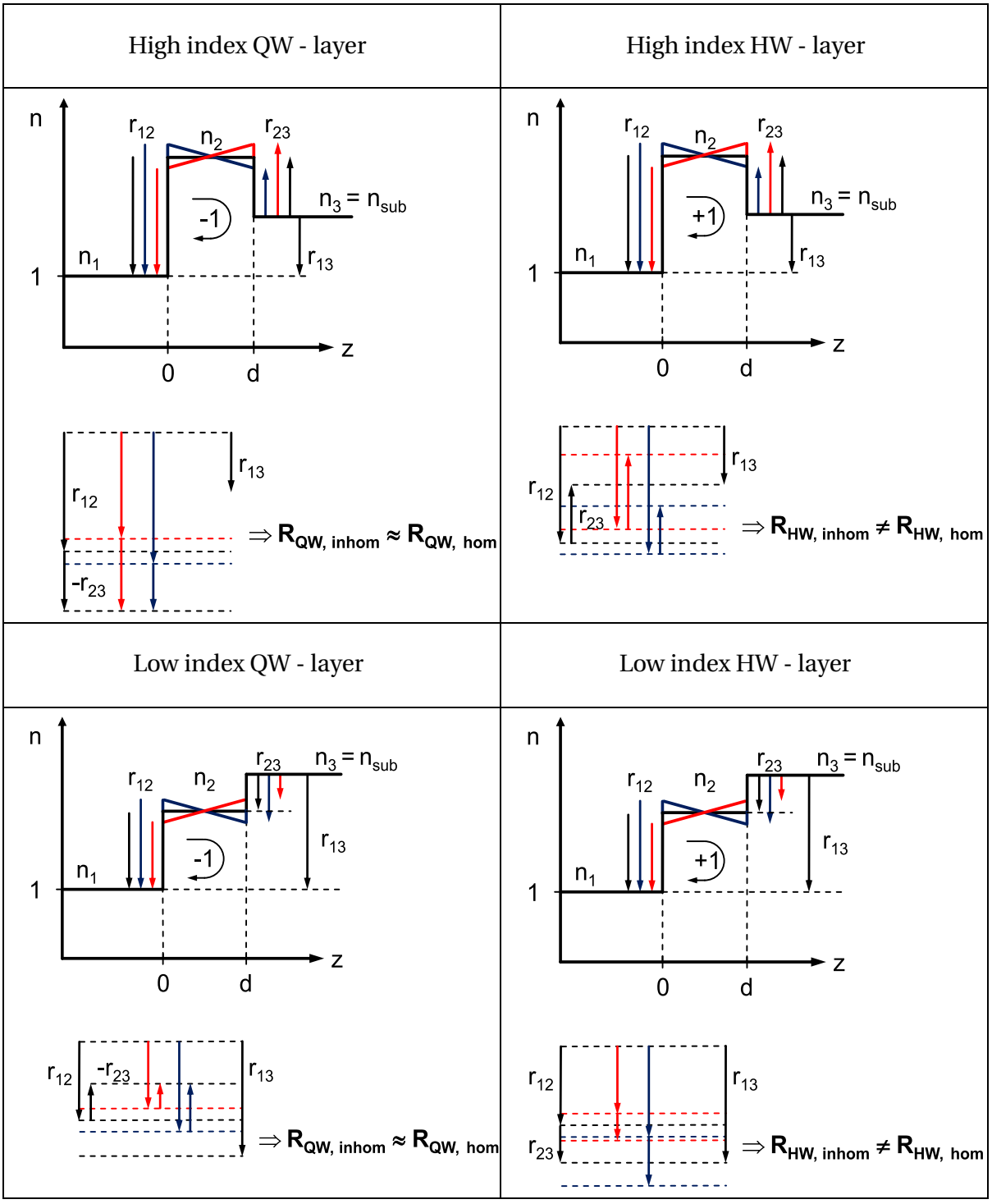

Figure 27: Illustration of the effect of negative (in red) and positive (in blue) index gradients of the reflectance in QW (left) and HW (right) point.

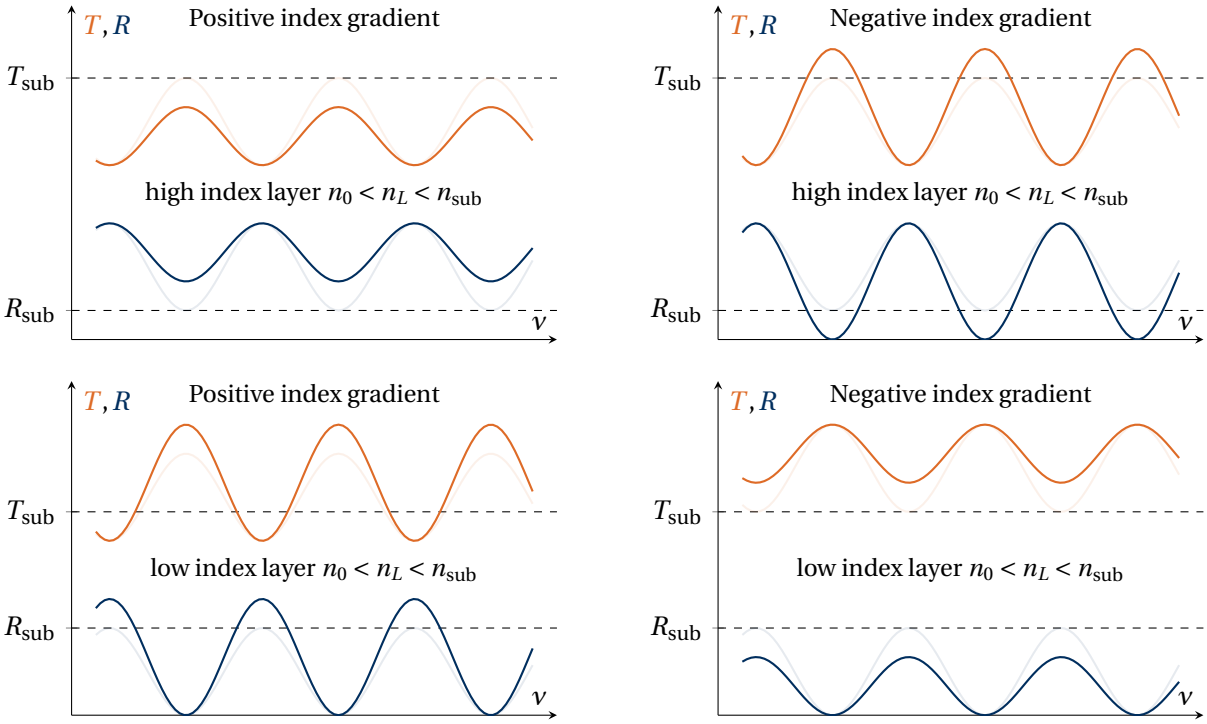

Figure 28: Left: Positive refractive index gradient. Right: Negative refractive index gradient.

We can see that the reflectivity scales linearly as a function of μ. We also find for $\mu \to 0$ that $r_{123} \to r_{13}$. We already showed in (5.22), that for a HW layer the transmittance and reflectivity is not dependent on medium 2.

We can repeat the same calculations now with a QW layer

$$r_{123,\mathrm{QW}} = \frac{r_{12} - r_{23}}{1 - r_{12} r_{23}} = \frac{(1 - \langle n\rangle + \mu)(\langle n\rangle + \mu + n_{\mathrm{sub}}) - (1 + \langle n\rangle - \mu)(\langle n\rangle + \mu - n_{\mathrm{sub}})}{(1 + \langle n\rangle - \mu)(\langle n\rangle + \mu + n_{\mathrm{sub}}) - (1 - \langle n\rangle + \mu)(\langle n\rangle + \mu - n_{\mathrm{sub}})}$$

terms $\langle n\rangle\,\mu, n_{\mathrm{sub}}\mu, \mu, \langle n\rangle, \langle n\rangle\, n_{\mathrm{sub}}$ cancel out

$$= \frac{n_{\mathrm{sub}} - \langle n\rangle^2 + \mu^2}{n_{\mathrm{sub}} + \langle n\rangle^2 - \mu^2}. \tag{5.40}$$

In contrast to the HW the reflectivity scales quadratically with μ. That is the reason why the QW points did not change in the vector diagrams in figure 27. For small μ the reflectivity is

$$r_{123,\mathrm{QW}} = \frac{n_{\mathrm{sub}} - \langle n\rangle^2}{n_{\mathrm{sub}} + \langle n\rangle^2}, \tag{5.41}$$

thus we can obtain information on $\langle n\rangle$. For $\langle n\rangle = \sqrt{1 - n_{\mathrm{sub}}}$ we would achieve ideal AR.

Now we return to the HW case and expand r_{123} for the case of $\mu \ll \langle n\rangle$

$$r_{123} \approx \left(r_{13} + \frac{\mu}{\langle n\rangle}\right)\left(1 - r_{13}\frac{\mu}{\langle n\rangle}\right) = r_{13} + \frac{\mu}{\langle n\rangle}\left(1 - r_{13}^2\right) = r_{13} + \frac{\mu}{\langle n\rangle} T_{\mathrm{sub}} + \mathcal{O}\left(\mu^2\right)$$

$$\Rightarrow R_{\mathrm{HW}} \approx R_{\mathrm{sub}} + \underbrace{2 r_{13} T_{\mathrm{sub}} \frac{\mu}{\langle n\rangle}}_{\Delta R}$$

$$R_{\mathrm{HW}} \approx R_{\mathrm{sub}} + 4 n_{\mathrm{sub}} \frac{1 - n_{\mathrm{sub}}}{(1 + n_{\mathrm{sub}})^3} \frac{2\mu}{\langle n\rangle}. \tag{5.42}$$

For $\Delta R < 0 (\mu > 0)$ we have a negative index gradient and vice versa. In conclusion, for small inhomogeneities, the QW points do not change and the HW points get modified by $\Delta R \propto \frac{\mu}{\langle n \rangle}$.

5.4 Thin film on thick substrates

So far we have only considered an infinitely thick substrate. However, in a real situation the substrate has a finite thickness. We assume a thick slab as our substrate. Then the transmittance is according to the incoherent case (5.7)

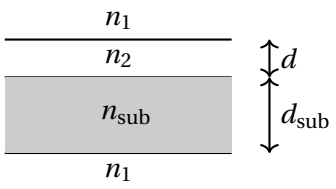

Figure 29: Thick substrate.

$$T = \frac{|t_{12}|^2 |t_{21}|^2 \exp\left(-\frac{2\omega}{c} d_s \operatorname{Im} \sqrt{\hat{n}_{\text{sub}}^2 - n_1^2 \sin^2\varphi}\right)}{1 - |r_{21}|^2 |r_{21}|^2 \exp\left(-\frac{4\omega}{c} d_s \operatorname{Im} \sqrt{\hat{n}_{\text{sub}}^2 - n_1^2 \sin^2\varphi}\right)}.$$

If we now place a thin film on the substrate the equation for the transmittance and reflectance modify to

$$\begin{aligned} T &= \frac{|t_{123}|^2 |t_{31}|^2 \exp\left(-\frac{2\omega}{c} d_s \operatorname{Im} \sqrt{\hat{n}_{\text{sub}}^2 - n_1^2 \sin^2\varphi}\right)}{1 - |r_{31}|^2 |r_{321}|^2 \exp\left(-\frac{4\omega}{c} d_s \operatorname{Im} \sqrt{\hat{n}_{\text{sub}}^2 - n_1^2 \sin^2\varphi}\right)} \\ R &= |r_{123}|^2 + \frac{|t_{123}|^2 |t_{321}|^2 |r_{31}|^2 \exp\left(-\frac{4\omega}{c} d_s \operatorname{Im} \sqrt{\hat{n}_{\text{sub}}^2 - n_1^2 \sin^2\varphi}\right)}{1 - |r_{31}|^2 |r_{321}|^2 \exp\left(-\frac{4\omega}{c} d_s \operatorname{Im} \sqrt{\hat{n}_{\text{sub}}^2 - n_1^2 \sin^2\varphi}\right)}, \end{aligned} \tag{5.43}$$

where the reflection r_{123} and transmission t_{123} coefficients are given by (5.9) and (5.10).

6 Wave propagation in stratified media

6.1 General theory for s-polarization

In the following we assume a so called *stratified medium* which has a dielectric constant $\varepsilon(z)$ only depending on z (c. f. figure 30 left). In order to derive the transmittance and reflectance we need to determine the electric fields E_e, E_r, E_t. For s-polarization we again assume $\boldsymbol{E} = E_y \hat{\mathbf{e}}_y$ and set the transmitted field $E_t = 1$.

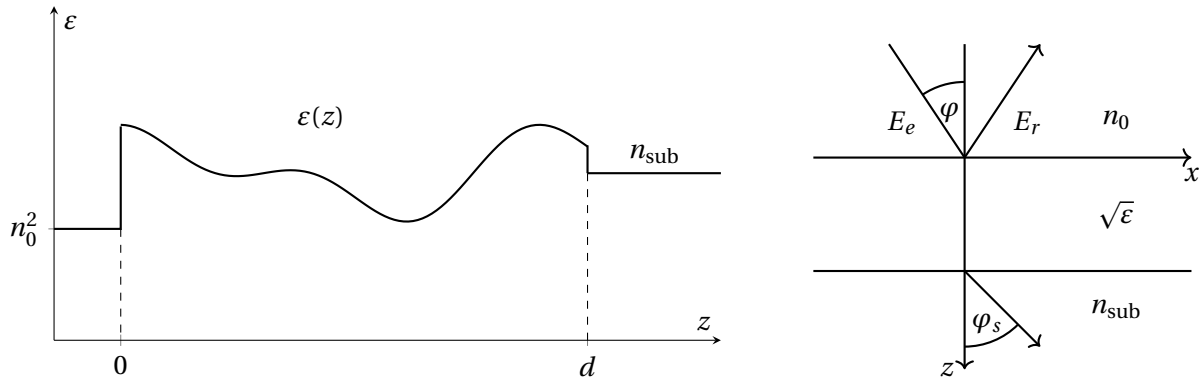

Figure 30: General scheme of a stratified media. We model the thinfilm with a dielectric constant which only depends on z. On the right side is a sketch of the geometry of the problem.

At $z = 0$ the total electric field is the superposition of incidence and reflected field $E_e + E_r = E(z = 0)$. The magnetic field $\boldsymbol{H}$ can be calculated as

$$\boldsymbol{H} = \frac{n}{\mu_0 c}\hat{\mathbf{e}} \times \boldsymbol{E} = \frac{n}{\mu_0 c}\begin{vmatrix} \hat{\mathbf{e}}_x & \hat{\mathbf{e}}_y & \hat{\mathbf{e}}_z \\ \sin\varphi & 0 & \pm\cos\varphi \\ 0 & E_y & 0 \end{vmatrix} \Rightarrow H_{x,e} = -\frac{n_0 \cos\varphi}{\mu_0 c} E_e, H_{x,r} = \frac{n_0 \cos\varphi}{\mu_0 c} E_r. \tag{6.1}$$

Then the total magnetic field at the boundary $Z = 0$ is

$$H_x(z = 0) = \frac{n_0 \cos\varphi}{\mu_0 c}(E_r - E_e) = \frac{n_0 \cos\varphi}{\mu_0 c}(E(z = 0) - 2E_e). \tag{6.2}$$

We can solve that equation for E_e and subsequently E_r to find the transmission/reflection coefficient

$$\begin{aligned} E_e &= \frac{1}{2}\left(E(z = 0) - \frac{\mu_0 c}{n_0 \cos\varphi} H_x(z = 0)\right) \\ &= \frac{1}{2n_0 \cos\varphi}\left(n_0 \cos\varphi E(z = 0) - \sqrt{\frac{\mu_0}{\varepsilon_0}} H_x(z = 0)\right) \\ \Rightarrow E_r = E(z = 0) - E_e &= \frac{1}{2n_0 \cos\varphi}\left(n_0 \cos\varphi E(z = 0) + \sqrt{\frac{\mu_0}{\varepsilon_0}} H_x(z = 0)\right). \end{aligned} \tag{6.3}$$

Then we can formulate the transmission and reflection coefficients for a stratified medium as

Reflection and transmission coefficients for a stratified medium

$$t = \frac{1}{E_0} = \frac{2n_0\cos\varphi}{n_0\cos\varphi E(z=0) - \sqrt{\frac{\mu_0}{\varepsilon_0}}H_x(z=0)} \tag{6.4}$$

$$r = \frac{E_r}{E_e} = \frac{n_0\cos\varphi E(z=0) + \sqrt{\frac{\mu_0}{\varepsilon_0}}H_x(z=0)}{n_0\cos\varphi E(z=0) - \sqrt{\frac{\mu_0}{\varepsilon_0}}H_x(z=0)}. \tag{6.5}$$

The means our task is now to calculate $E(z=0)$ and $H_x(z=0)$ at the boundary. We can do that by finding solutions of MAXWELL's equations

$$\boldsymbol{E}(\boldsymbol{r},t) = \boldsymbol{E}_0(\boldsymbol{r})\mathrm{e}^{-\mathrm{i}\omega t}, \qquad \boldsymbol{H}(\boldsymbol{r},t) = \boldsymbol{H}_0(\boldsymbol{r})\mathrm{e}^{-\mathrm{i}\omega t}. \tag{6.6}$$

First we make use of FARADAY's law

$$\vec{\boldsymbol{\nabla}} \times \boldsymbol{E} = -\frac{\partial}{\partial t}\boldsymbol{B} = \mathrm{i}\omega\mu_0\boldsymbol{H} \tag{6.7}$$

$$\text{also} \quad \vec{\boldsymbol{\nabla}} \times \boldsymbol{E} = \begin{vmatrix} \hat{\mathbf{e}}_x & \hat{\mathbf{e}}_y & \hat{\mathbf{e}}_z \\ \partial x & \partial y & \partial z \\ 0 & E_y & 0 \end{vmatrix} = \frac{\partial E_y}{\partial x}\hat{\mathbf{e}}_z - \frac{\partial E_y}{\partial z}\hat{\mathbf{e}}_x \quad \Rightarrow \quad \boldsymbol{H} = \begin{pmatrix} H_x \\ 0 \\ H_z \end{pmatrix}.$$

Comparing both results we find

$$\mathrm{i}\omega\mu_0 H_x = -\frac{\partial}{\partial z}E_y \tag{6.8a}$$

$$\mathrm{i}\omega\mu_0 H_Z = +\frac{\partial}{\partial x}E_y. \tag{6.8b}$$

We can do the same steps with AMPERE's law as well

$$\vec{\boldsymbol{\nabla}} \times \boldsymbol{H} = \frac{\partial}{\partial t}\boldsymbol{D} = -\mathrm{i}\omega\varepsilon\varepsilon_0\boldsymbol{E} \tag{6.9}$$

$$\text{also} \quad \vec{\boldsymbol{\nabla}} \times \boldsymbol{H} = \begin{vmatrix} \hat{\mathbf{e}}_x & \hat{\mathbf{e}}_y & \hat{\mathbf{e}}_z \\ \partial x & \partial y & \partial z \\ H_x & 0 & H_z \end{vmatrix} = \left(\frac{\partial H_x}{\partial z} - \frac{\partial H_z}{\partial x}\right)\hat{\mathbf{e}}_y \quad \Rightarrow \quad \mathrm{i}\omega\varepsilon\varepsilon_0 E_y = \frac{\partial H_z}{\partial x} - \frac{\partial H_x}{\partial z}. \tag{6.10}$$

Now we may calculate $\frac{\partial}{\partial x}$(6.8b) $-$ $\frac{\partial}{\partial z}$(6.8a)

$$\left(\frac{\partial^2}{\partial x^2} + \frac{\partial^2}{\partial z^2}\right)E_y = \mathrm{i}\omega\mu_0\left(\frac{\partial H_z}{\partial x} - \frac{\partial H_x}{\partial z}\right) \overset{(6.10)}{=} -k_0^2\varepsilon(z)E_y. \tag{6.11}$$

Now we do a separation ansatz for $E_y = X(x)U(z)$

$$\begin{aligned} U\frac{\mathrm{d}^2}{\mathrm{d}x^2}X + X\frac{\mathrm{d}^2}{\mathrm{d}z^2} &= -k_0^2\varepsilon(z)U\cdot X \\ \Rightarrow \underbrace{\frac{1}{X}\frac{\mathrm{d}^2}{\mathrm{d}x^2}X}_{\text{only } f(x)} &= \underbrace{-\frac{1}{U}\frac{\mathrm{d}^2}{\mathrm{d}z^2}U - k_0^2\varepsilon(z)}_{\text{only } f(z)} \equiv -k_0^2\xi^2 = \text{const.} \end{aligned} \tag{6.12}$$

Then we can solve the x dependent part of the differential equation easily

$$X(x) = \mathrm{e}^{\mathrm{i}k_0\xi x} \quad \text{and} \quad E_y = U(z)\mathrm{e}^{\mathrm{i}k_0\xi x}. \tag{6.13}$$

Now we proceed by trying to find an expression of H_x using (6.8a)

$$H_x = -\frac{1}{\mathrm{i}\omega\mu_0}\frac{\partial E_y}{\partial z} = -\underbrace{\frac{1}{\mathrm{i}\omega\mu_0}\frac{\partial U}{\partial z}}_{:=V(z)}\mathrm{e}^{\mathrm{i}k_0\xi x} = -V(z)\mathrm{e}^{\mathrm{i}k_0\xi x}$$

$$\frac{\partial H_x}{\partial z} = -\frac{\mathrm{d}V}{\mathrm{d}z}\mathrm{e}^{\mathrm{i}k_0\xi x} \overset{(6.10)}{=} \frac{\partial H_z}{\partial x} - \mathrm{i}\omega\varepsilon\varepsilon_0 E_y \overset{(6.8b)}{=} \left[-\frac{k_0\xi^2}{\mathrm{i}\omega\mu_0} - \mathrm{i}\omega\varepsilon\varepsilon_0\right]E_y. \tag{6.14}$$

Then using $E_y = U\mathrm{e}^{\mathrm{i}k_0\xi x}$ we find

$$\frac{\mathrm{d}V}{\mathrm{d}z} = \mathrm{i}\omega\varepsilon_0\left[\varepsilon(z) - \frac{k_0^2\xi^2}{\omega^2\mu_0\varepsilon_0}\right]U = \mathrm{i}\omega\varepsilon_0(\varepsilon(z) - \xi^2)U. \tag{6.15}$$

In order to have the same dimensions for U and V we perform a substitution $u = U$ and $v = \sqrt{\frac{\varepsilon_0}{\mu_0}}V$

$$\frac{\mathrm{d}U}{\mathrm{d}z} = \frac{\mathrm{d}u}{\mathrm{d}z} = \mathrm{i}\omega\mu_0 V(z) = \mathrm{i}\omega\sqrt{\varepsilon_0\mu_0}v = \mathrm{i}k_0 v. \tag{6.16}$$

This leads to the following coupled equations for $u(z)$ and $v(z)$

$$\frac{\mathrm{d}v}{\mathrm{d}z} = \mathrm{i}k_0(\varepsilon(z) - \xi^2)u \quad \text{and} \quad \frac{\mathrm{d}u}{\mathrm{d}z} = \mathrm{i}k_0 v, \quad \xi = n_0\sin\varphi. \tag{6.17}$$

Since in the homogeneous media n_0 we can write $E_y = U(z)\mathrm{e}^{\mathrm{i}k_x x}$ we can identify here $k_0\xi = k_x = \frac{\omega}{c}n_0\sin\varphi$. Furthermore we know that ξ^2 is a constant quantity which means

$$k_0\xi = \frac{\omega}{c}n_{\text{sub}}\sin\varphi_s \quad \Rightarrow n_0\sin\varphi = n_{\text{sub}}\sin\varphi_s \quad \text{Snell's law.} \tag{6.18}$$

Now we can formulate our boundary conditions at $z = 0$. From our assumption $E_t = 1$ we immediately follow $u(z = d) = 1$. Then the magnetic field is

$$H_x(z = d) = -\frac{n_{\text{sub}}\cos\varphi_s}{\mu_0 c}$$

$$\Rightarrow v(z = d) = \sqrt{\frac{\mu_0}{\varepsilon_0}}\frac{n_{\text{sub}}\cos\varphi_s}{\mu_0 c} = n_{\text{sub}}\cos\varphi_s \quad \text{and} \quad u(z = d) = 1. \tag{6.19}$$

Now we can substitute u and v for E_y and H_x, H_z in (6.4) and (6.5)

Transmission and reflection coefficients for the normalized fields

$$t = \frac{2n_0\cos\varphi}{n_0\cos\varphi u_0 + v_0} \qquad T = \frac{n_{\text{sub}}\cos\varphi_s}{n_0\cos\varphi}|t|^2 \tag{6.20}$$

$$r = \frac{n_0\cos\varphi u_0 - v_0}{n_0\cos\varphi u_0 + v_0} \qquad R = |r|^2. \tag{6.21}$$

6.2 Matrix formalism

Since we now know the transmission and reflection coefficients for the fields at the boundary u_0 and v_0 but our fields are given as $u(z=0)$ and $v(z=0)$ we need to find a way to relate them to each other using the equations (6.17).

6.2.1 Characteristic matrix

In the following we assume two different solutions of our system namely

$$\begin{aligned} u_1, v_1: &\quad u_1(z=0)=1, v_1(z=0)=0 \\ u_2, v_2: &\quad u_2(z=0)=0, v_2(z=0)=1. \end{aligned} \tag{6.22}$$

Both solutions have to fulfill (6.17)

$$\begin{aligned} \frac{\mathrm{d}u_1}{\mathrm{d}z} &= \mathrm{i}k_0 v_1 \quad \Big| \cdot v_2, & \frac{\mathrm{d}v_1}{\mathrm{d}z} &= \mathrm{i}k_0(\varepsilon(z)-\xi^2)u_1 \quad \Big| \cdot u_2 \\ \frac{\mathrm{d}u_2}{\mathrm{d}z} &= \mathrm{i}k_0 v_2 \quad \Big| \cdot v_1, & \frac{\mathrm{d}v_2}{\mathrm{d}z} &= \mathrm{i}k_0(\varepsilon(z)-\xi^2)u_2 \quad \Big| \cdot u_1. \end{aligned} \tag{6.23}$$

If we now subtract both differential equations we find

$$\left.\begin{aligned} \frac{\mathrm{d}u_1}{\mathrm{d}z}v_2 - \frac{\mathrm{d}u_2}{\mathrm{d}z}v_1 = 0 \\ \frac{\mathrm{d}v_2}{\mathrm{d}z}u_1 - \frac{\mathrm{d}v_1}{\mathrm{d}z}u_2 = 0 \end{aligned}\right\} \Rightarrow \frac{\mathrm{d}}{\mathrm{d}z}(u_1 v_2 - v_1 u_2) = 0. \tag{6.24}$$

This means $u_1 v_2 - v_1 u_2 = \text{const.} = 1$, which can be determined by evaluating the functions at $z=0$.

An arbitrary solution $u(z), v(z)$ with the boundary conditions $u(0)=u_0, v(0)=v_0$ can be constructed as follows

$$u(z) = u_0 u_1(z) + v_0 u_2(z) \quad \text{and} \quad v(z) = u_0 v_1(z) + v_0 v_2(z). \tag{6.25}$$

We can also write this system of equations in matrix form

$$\begin{pmatrix} u(z) \\ v(z) \end{pmatrix} = \underbrace{\begin{pmatrix} u_1 & u_2 \\ v_1 & v_2 \end{pmatrix}\begin{pmatrix} u_0 \\ v_0 \end{pmatrix}}_{\hat{m}^{-1}} \quad \Rightarrow \quad \begin{pmatrix} u_0 \\ v_0 \end{pmatrix} = \underbrace{\begin{pmatrix} v_2 & -u_2 \\ -v_1 & u_1 \end{pmatrix}}_{\hat{m}\text{ characteristic matrix}} \begin{pmatrix} u(z) \\ v(z) \end{pmatrix}. \tag{6.26}$$

The matrix $\hat{m}$ is the *characteristic matrix* of the stratified medium. As shown in (6.24) it has a determinant of one. If we know $u(z=d), v(z=d)$ at the substrate we can determine u_0 and v_0 using the characteristic matrix.

For a stratified medium with a generic dielectric constant $\varepsilon(z)$ we can replace its profile with a piecewise constant function. Then we can calculate the characteristic matrix of every single homogeneous layer to determine u_0, v_0.

6.2.2 Characteristic matrix of a single homogeneous film

First we want to discuss the structure of the characteristic matrix for a single, homogeneous film. We can write the expression $\varepsilon - \xi^2$ in equation (6.17) as

$$\varepsilon - \xi^2 = \varepsilon - n_0^2 \sin^2\varphi = \hat{n}^2 - \hat{n}^2 \sin^2\psi = \hat{n}^2 \cos\psi, \tag{6.27}$$

where ψ is the propagation angle in the homogeneous film. Taking the derivative of (6.17) leads to the following equations

$$\left.\begin{aligned} \frac{\mathrm{d}^2 u}{\mathrm{d}z^2} + k_0^2 \hat{n}^2 \cos^2\psi\, u = 0 \\ \frac{\mathrm{d}^2 v}{\mathrm{d}z^2} + k_0^2 \hat{n}^2 \cos^2\psi\, v = 0 \end{aligned}\right\} \Rightarrow \text{solutions: } \sin\delta, \cos\delta \quad \text{with} \quad \delta = k_0 \hat{n} \cos\psi z. \tag{6.28}$$

Matching with the initial conditions (6.22) we can choose

$$\begin{aligned} u_1 = \cos\delta \quad &\Rightarrow \quad \frac{\mathrm{d}u_1}{\mathrm{d}z} = -\sin\delta\, k_0 \hat{n} \cos\psi \overset{(6.17)}{=} \mathrm{i} k_0 v_1 \\ \Rightarrow v_1 = \mathrm{i} n \cos\psi \sin\delta & \end{aligned} \tag{6.29}$$

$$\begin{aligned} \text{and} \quad v_2 = \cos\delta \quad &\Rightarrow \quad \frac{\mathrm{d}v_2}{\mathrm{d}z} = -k_0 \hat{n} \cos\psi \overset{(6.17)}{=} \mathrm{i} k_0 \overbrace{(\varepsilon(z) - \xi^2)}^{=\hat{n}^2\cos^2\psi} u \\ \Rightarrow u_2 = \frac{\mathrm{i}}{\hat{n}\cos\psi} \sin\delta. & \end{aligned} \tag{6.30}$$

We can combine these results into the characteristic matrix of a homogeneous film

Characteristic matrix of a single homogeneous film

$$\hat{m} = \begin{pmatrix} v_2 & -u_2 \\ -v_1 & u_1 \end{pmatrix} = \begin{pmatrix} \cos\delta & -\frac{\mathrm{i}}{\hat{n}\cos\psi}\sin\delta \\ -\mathrm{i} n \cos\psi \sin\delta & \cos\delta \end{pmatrix} \quad \delta = 2\pi\nu\sqrt{\hat{n}^2 - n_0^2 \sin^2\varphi}. \tag{6.31}$$

6.2.3 Characteristic matrix of a film stack

For a film stack the characteristic matrix is simply given by the product of the matrices of the single layer stacks

$$\begin{pmatrix} u_0 \\ v_0 \end{pmatrix} = \prod_{j=1}^{N} \hat{m}_j(d_j) \begin{pmatrix} u(z=d) \\ v(z=d) \end{pmatrix}. \tag{6.32}$$

Using the boundary conditions (6.19) for $u(z=d)$ and $v(z=d)$ we have

$$\begin{pmatrix} u_0 \\ v_0 \end{pmatrix} = \begin{pmatrix} m_{11} & m_{12} \\ m_{21} & m_{22} \end{pmatrix} \begin{pmatrix} 1 \\ n_{\mathrm{sub}} \cos\varphi_s \end{pmatrix}. \tag{6.33}$$

This means the fields at $z = 0$ are given as

$$u_0 = m_{11} + m_{12} n_{\text{sub}} \cos\varphi_s \tag{6.34}$$
$$v_0 = m_{21} + m_{22} n_{\text{sub}} \cos\varphi_s \tag{6.35}$$

Example 1: Single interface

For a single interface we have $\delta = 0$ and thus $\hat{m} = \mathbb{1}$ leading to

$$r_s = \frac{n_0 \cos\varphi - n_{\text{sub}} \cos\varphi_s}{n_0 \cos\varphi + n_{\text{sub}} \cos\varphi_s} \quad \Rightarrow \quad \text{Fresnel's equation.} \tag{6.36}$$

Example 2: Single quarter wave layer

We assume a single QW layer with real n at normal incidence. With $\delta = \frac{\pi}{2}$ we find

$$\hat{m}_{QW} = \begin{pmatrix} 0 & -\frac{\mathrm{i}}{n} \\ -\mathrm{i}n & 0 \end{pmatrix} \quad \text{and} \quad r_s = \frac{n_0 \cos\varphi(-\frac{\mathrm{i}}{n} n_{\text{sub}}) + \mathrm{i}n}{n_0 \cos\varphi(-\frac{\mathrm{i}}{n} n_{\text{sub}}) - \mathrm{i}n} = \frac{n_0 n_{\text{sub}} - n^2}{n_0 n_{\text{sub}} + n^2}. \tag{6.37}$$

As before, we see that for $n = \sqrt{n_0 n_{\text{sub}}}$ a single layer AR coating can be realized.

Example 3: QW stack

We now examine a QW-stack with real n at n. i. The layout $n_0|(LH)^N|n_{\text{sub}}$ gives us

$$\hat{M} = (\hat{m}_L \cdot \hat{m}_H)^N = \left[\begin{pmatrix} 0 & -\frac{\mathrm{i}}{n_L} \\ -\mathrm{i}n_L & 0 \end{pmatrix} \begin{pmatrix} 0 & -\frac{\mathrm{i}}{n_H} \\ -\mathrm{i}n_H & 0 \end{pmatrix} \right]^N = \begin{pmatrix} \left(-\frac{n_H}{n_L}\right)^N & 0 \\ 0 & \left(-\frac{n_L}{n_H}\right)^N \end{pmatrix} \tag{6.38}$$

$$r_s = \frac{n_0 \left(-\frac{n_L H}{n_L}\right)^N - \left(-\frac{n_L}{n_H}\right)^N n_{\text{sub}}}{n_0 \left(-\frac{n_L H}{n_L}\right)^N + \left(-\frac{n_L}{n_H}\right)^N n_{\text{sub}}} = \frac{n_0 - \left(-\frac{n_L}{n_H}\right)^{2N} n_{\text{sub}}}{n_0 + \left(-\frac{n_L}{n_H}\right)^{2N} n_{\text{sub}}} \overset{N\to\infty}{\to} 1. \tag{6.39}$$

The special case $N = 0$ reproduces the reflectivity of a single interface. For $N = 1$

$$r_{N=1} = \frac{n_0 - \left(-\frac{n_L}{n_H}\right)^2 n_{\text{sub}}}{n_0 + \left(-\frac{n_L}{n_H}\right)^2 n_{\text{sub}}} \quad \Rightarrow r \overset{?}{=} 0 \Rightarrow n_0 = \left(\frac{n_L}{n_H}\right)^2 n_{\text{sub}}. \tag{6.40}$$

We can rewrite the condition for AR as

$$\frac{n_H}{n_L} = \sqrt{\frac{n_{\text{sub}}}{n_0}} \quad \text{V-coating.} \tag{6.41}$$

The particular case of $n_H = n - L$ results in

$$r_{N=1} = \frac{n_0 - n_{\text{sub}}}{n_0 + n_{\text{sub}}} \quad \text{HW layer.} \tag{6.42}$$

We can see that two QW layers with same refractive index result in a HW layer (for arbitrary N).

7 QW-stacks and derived systems

7.1 QW at normal incidence

We now want to consider the following kind of quarter wave stack

$$\text{air}|H(LH)^N|\text{sub} \quad \text{with} \quad n_H d_H = n_L d_L = \frac{\lambda_0}{4}, \tag{7.1}$$

where λ_0 is the central rejection wavelength. The corresponding rejection band is displayed in figure 31. We can see that for every $\Delta\nu = 2/\lambda_0$ the pattern of the rejection band repeats. We can explicitly calculate that via

$$\delta_1 = 2\pi\nu_1 nd \quad \Rightarrow \quad \Delta\delta = 2\pi\Delta\nu nd = \frac{4\pi nd}{4nd} = \pi. \tag{7.2}$$

This means $\sin(\delta_1 + \Delta\delta) = -\sin(\delta_1)$ and analogously $\cos(\delta_1 + \Delta\delta) = -\cos(\delta_1)$. This means the reflection coefficient is changed by its sign, however, the reflectivity is the same.

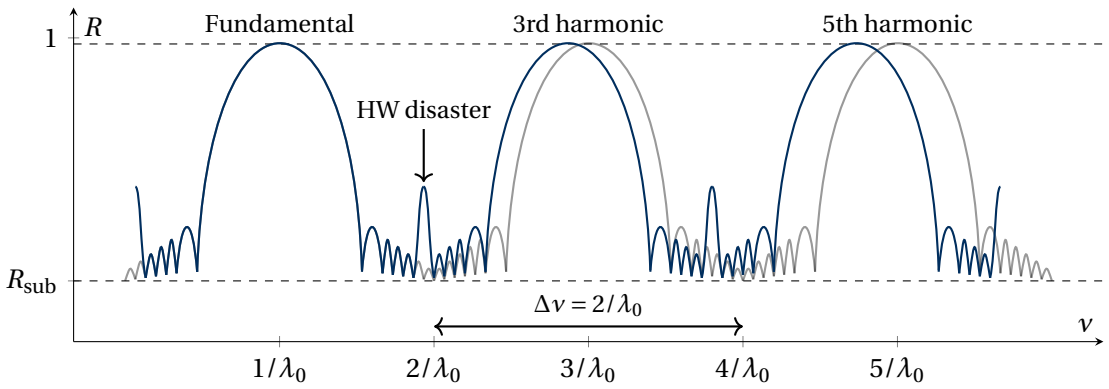

Figure 31: Rejection band of a QW stack with (blue) and without (grey) dispersion. For a dispersive material we observe increased reflectivity at the HW points (even harmonics). This is called *Halfwave disaster*.

The width of the rejection band is dependent on the refractive index difference of the low and high index medium. For increasing refractive index difference the rejection band gets broader. We can formulate that without proof as

$$\Delta\lambda\Big|_{\lambda_0} = \frac{4\lambda_0}{\pi}\arcsin\left(\frac{n_H - n_L}{n_H + n_L}\right). \tag{7.3}$$

Furthermore we want to mention that the number of minima between adjacent odd rejection zones is equal to the number of layers $2N+1$.

Now we also want to consider the effects of material dispersion. For no-absorption we have normal dispersion meaning that $\frac{\mathrm{d}n}{\mathrm{d}\nu} > 0$. Let us consider the QW and HW points

$$\left.\begin{aligned} n_{\text{QW}} d &= \tfrac{\lambda_{\text{QW}}}{4} \\ n_{\text{HW}} d &= \tfrac{\lambda_{\text{HW}}}{2} \end{aligned}\right\} \Rightarrow d = \frac{\lambda_{\text{QW}}}{4n_{\text{QW}}} = \frac{\lambda_{\text{HW}}}{2n_{\text{HW}}}. \tag{7.4}$$

Finally we obtain

$$\lambda_{\mathrm{HW}} = \underbrace{\frac{n_{\mathrm{HW}}}{n_{\mathrm{QW}}}}_{>1} \frac{\lambda_0}{2} \quad \Rightarrow \lambda_{\mathrm{HW}} > \frac{\lambda_0}{2} \quad \text{or} \quad \frac{1}{\lambda_{\mathrm{HW}}} < \frac{2}{\lambda_0}. \tag{7.5}$$

We observe that the periodicity in the reflectivity breaks down. We find the maximum of the next QW or HW point at lower wave numbers as indicated in figure 31.

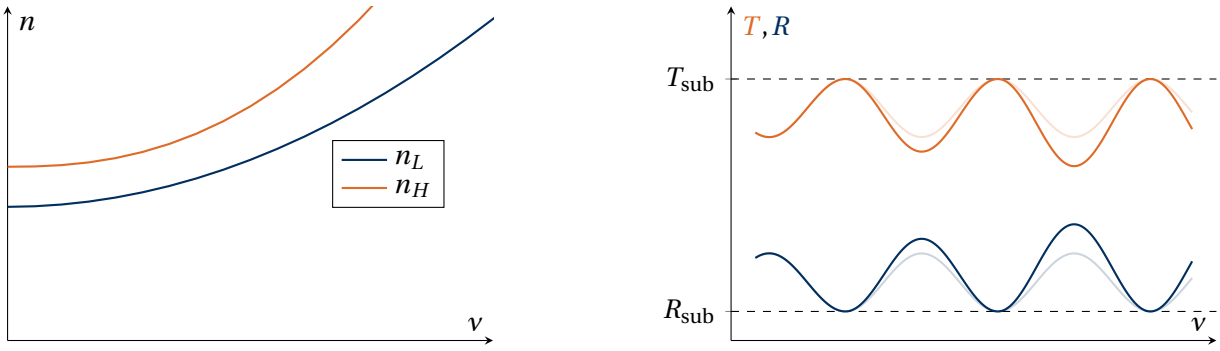

Figure 32: Left: Normal dispersion of materials. Typically, the dispersion is stronger for high index materials. This effect causes the appearance of the HW disaster.
Right: Dispersion in a single high index layer. For higher wavenumbers the index contrast gets larger, thus increasing the reflectivity at the QW points.

We can explain the effect of the HW disaster using figure 32. The wavelength at the HW points is given by

$$\lambda_{\mathrm{HW,L}} = \frac{n_{\mathrm{HW,L}}}{n_{\mathrm{QW,L}}} \frac{\lambda_0}{2}, \quad \lambda_{\mathrm{HW,H}} = \frac{n_{\mathrm{HW,H}}}{n_{\mathrm{QW,H}}} \frac{\lambda_0}{2}. \tag{7.6}$$

However, since the ratios $\frac{n_{\mathrm{HW,L}}}{n_{\mathrm{QW,L}}}$ and $\frac{n_{\mathrm{HW,H}}}{n_{\mathrm{QW,H}}}$ are not the same, the HW points will be different for low and high index layer.

7.2 Derived systems

Bragg reflectors

We will now come back to the picture of refractive index profiles. A QW stack is only a single example of a periodic modulation of the optical properties of the medium in space. In fact, any periodic modulation, no matter whether it corresponds to a QW stack or some different periodicity will be accompanied by what we call rejection zones. We can compare this to the propagation of charged carriers in crystals where we also have allowed and forbidden zones of kinetic energy.

We can now define a BRAGG reflector as

$$n_H d_H + n_L d_L = \frac{\lambda_0}{2} \quad \text{but} \quad n_H d_H \neq n_L d_L. \tag{7.7}$$

This means that high and low index layers appear to have different optical thickness. Analogously as for dispersion the optical thickness does not coincide at the HW points which means we find rejection zones at all harmonics of the fundamental wavelength $\lambda_0, \frac{\lambda_0}{2}, \frac{\lambda_0}{3}, \ldots$.

Rugate filter

For a Rugate filter we no more require that we have a piecewise constant refractive index but rather a continuous, periodic distribution. We now generalize the reflectivity condition to

$$\langle n \rangle \Lambda = \frac{\lambda_0}{2}, \tag{7.8}$$

where Λ is the spatial period of the refractive index profile (c. f. figure 33). We will have rejection at $\lambda_0, \frac{\lambda_0}{2}, \frac{\lambda_0}{3}, \ldots$, but the intensity drops down quickly with increasing order. The explanation of the decrease of efficiency in reflection is given by the lack of a sharp interface. In fact, since the refracted index is modulated continously we do not have a infinitesimally thin interface. For the efficiency the relation between the wavelength λ_0 and the region where the refractive index is changing matters. For large wavelengths λ this relation is small so the reflectivity might be close to the Bragg reflector. However, for smaller wavelengths the interfaces looks like a refractive index gradient. The lower the steepness of this gradient, the smaller is the efficiency to provide a reflection. Thus the rejection zones become weaker. However, the construction of a rugate filter is more difficult than of a Bragg reflector.

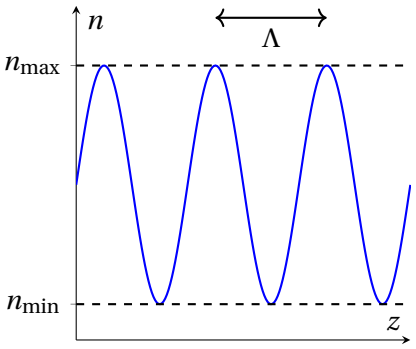

Figure 33: Rugate filter.

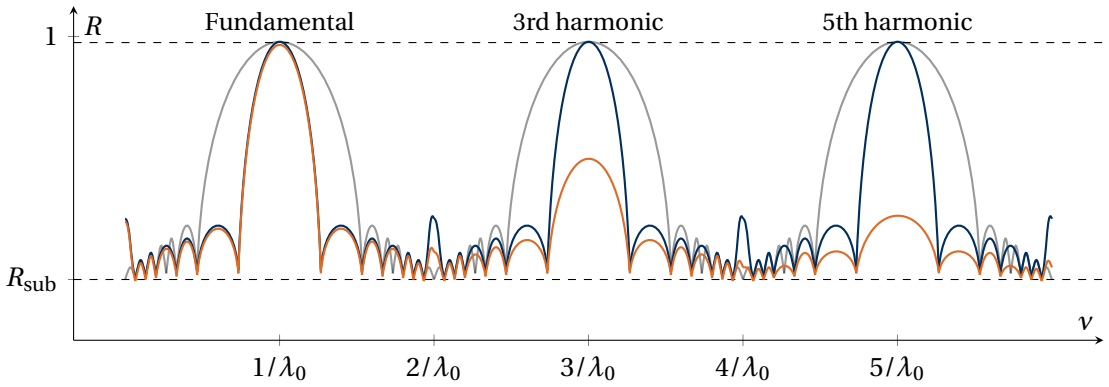

Figure 34: Rejection band of a Bragg reflector (blue) and a rugate filter (orange). For both reflectors we have a narrower rejection band than in the QW stack (grey). In the rugate filter higher orders of reflection are weaker than the fundamental.

Mirrors for ultrashort pulses

In the following we want to consider ultrashort pulses. If we assume a short pulse with pulse length τ, the spectrum is given by the Fourier transform of the temporal electric field. Due to the time-bandwidth product of the Fourier transform the spectral bandwidth of the pulse is cloesely related to the pulse length via $\tau \cdot \Delta\omega \geq$ const. Generally, the shorter the pulse, the broader the spectrum.

For the design of mirrors for ultrashort pulses our first traget is a broadband reflection. Secondly we also want to control the phase behaviour, since a pulse travelling through a dispersive medium is broadened. Since the reflection coefficient $r = |r|e^{i\delta_r}$ is a complex value we

have requirements on $|r|$ and δ_r which leads us to the design of so called *dispersive mirrors*. The historically first approach was the design of a chirped mirror displayed in figure 35.

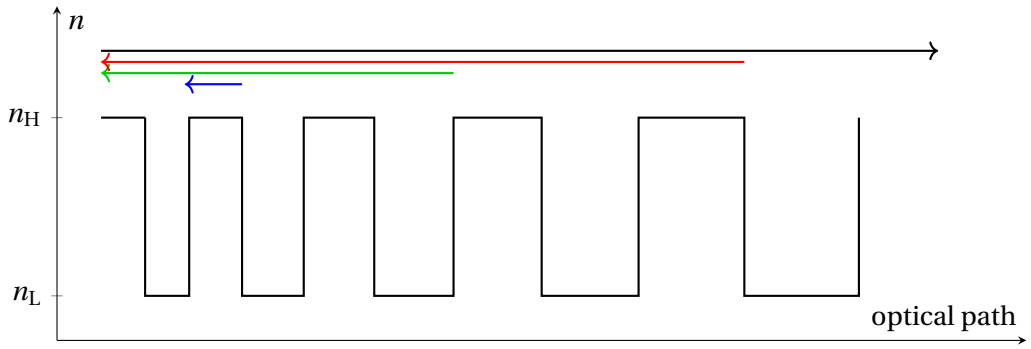

Figure 35: Design of a chirped mirror. The QW condition for AR is fulfilled for different wavelengths in certain depths. A chirped mirror can be used to compensate normal dispersion by increasing the path length for the red components of the light.

Furthermore we have to consider the significance of nonlinear-optical-processes e. g. two photon absorption (TPA). For lower pulse lengths the maximum of the electric field strength rises until we reach a regime, where nonlinear effects come into play.

8 Remarks on Coating Design

The idea of design is to find one that fits a required specification, i. e. we have to fulfill a spectral target $R(\lambda), T(\lambda), A(\lambda)$.

> If the spectral target includes only normal or oblique incidcence with s-polarization and no absorption, then a design built from two materials only but with largest refractive index contrast is favorable.

We also note that for a design task one should always consider both interfaces (front and back of the substrate).

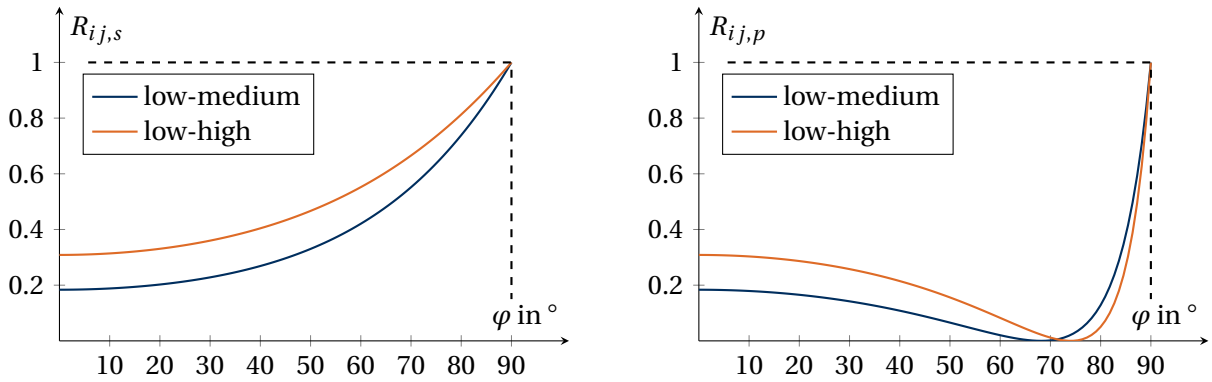

Figure 36: Reflectivity R for s-polarization (left) and p-polarization (right). If we compare the reflectivity for a low-high inteface and a low-medium interface, we can see that for s-polarization the reflectivity is always higher and thus this layer is preferable for design. For p-polarization it gets more complicated. One might include materials with intermediate refractive indices.

These days the design task is most often performed by computers where we can define an initial design and the computer performs numerical refinement procedures, by e. g. using *merit functions*

$$MF = \sum_j \left(\frac{R_{\text{target}}(\lambda_j) - R_{\text{calc}}(\lambda_j, \{n(\lambda_j)\}, \{n(d_j)\})}{\delta R(\lambda_j)} \right)^2 . \tag{8.1}$$

Finally we now also want to discuss several design specifications:

Anti reflective coating

For an AR-coating we may simply use a low-index layer. If we do not have a low index layer available, we might use a QW stack. However, we must ensure that the AR spectral range fits in-between the first and third harmonic rejection zone.

High reflective coating

We can achieve a HR-coating with a QW stack in the fundamental rejection zone. The higher the number of periods, the higher the maximum reflectivity will be. Otherwise we can also utilize a chirped design or a metal coating.

Neutral beam splitter (NBS)

We can realize a neutral beams splitter with a QW stack with only a few periods.

Short/long pass filter

We can design long and short pass filters in the following way:

$$\begin{aligned} \text{short pass filter:} \quad & \text{air } |0.5\text{LH}(\text{LH})^N 0.5\text{L}| \text{ sub} \\ \text{long pass filter:} \quad & \text{air } |0.5\text{HL}(\text{HL})^N 0.5\text{H}| \text{ sub.} \end{aligned} \tag{8.2}$$

We can realize this by coating the front of the substrate with the long pass filter and the back side with a short pass filter.

Polarizing beam splitter

For the design of a polarizing bema splitter we can use the fact that for oblique incidence the width of the rejection zone is larger for s-polarization than for p-polarization. At the edge of the rejection zone we can design a layer transmitting p-polarized light while reflecting s-polarized light.

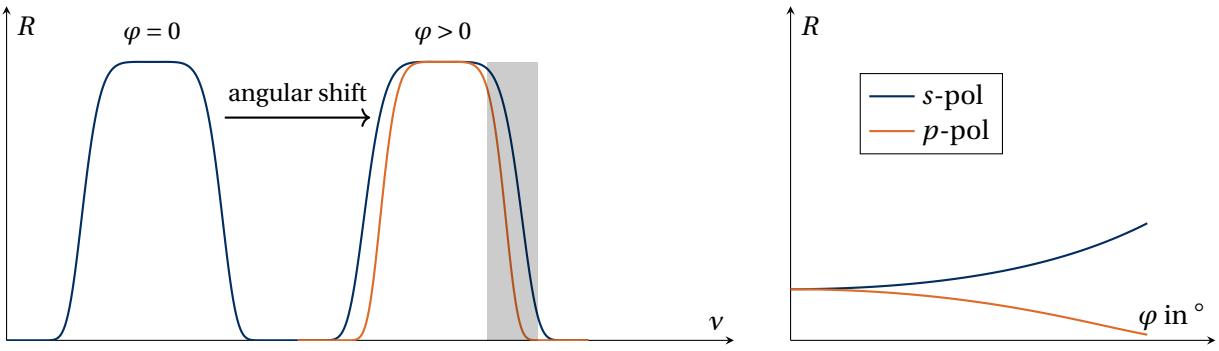

Figure 37: Left: Rejection zones for s-polarization and p-polarization for normal and oblique incidence. We can design a beam splitter at the edge of the rejection zone.
Right: Angular dependence of the reflectance for s- and p-polarization.

Absorber

For an absorber we need to maximize $A = 1 - R - T$. As a substrate we wanna choose a high absorbing material. However, we must also consider reducing the reflectivity of the surface of the substrate. For that we would also apply an AR-coating.

Narrow band pass filter

A narrow band pass filter (NBP) (assuming $A = 0$) can be designed by a QW-stack in a HW-layer design where we insert an additional high index layer in the middle of the stack (c. f. equation (5.18))

$$\text{air}|(\text{HL})^N\text{HH}(\text{LH})^N|\text{sub}\Big|_{\lambda_0} = \text{air}|\text{sub}. \tag{8.3}$$

The corresponding characteristic matrix is then

$$\hat{M} = \begin{pmatrix} \left(-\frac{n_L}{n_H}\right)^N & 0 \\ 0 & \left(-\frac{n_H}{n_L}\right)^N \end{pmatrix} \begin{pmatrix} -1 & 0 \\ 0 & -1 \end{pmatrix} \begin{pmatrix} \left(-\frac{n_H}{n_L}\right)^N & 0 \\ 0 & \left(-\frac{n_L}{n_H}\right)^N \end{pmatrix} = \begin{pmatrix} -1 & 0 \\ 0 & -1 \end{pmatrix}. \tag{8.4}$$

At the fundamental wavelength we will have minimal reflection, whereas around λ_0 we have the rejection band of the QW stack. The physical reason is the destructive interference of the reflected beams in the HW-layer. We can reduce the spectral bandwith of the NBP by increasing the life time in the mirror cavity. This can be achieved by increasing the number of layers N.

For maximum transmission we might additionally include matching layers

$$\text{air}|\text{matching 1}|M_1|C_1|M_2|C_2|\ldots|M_N|\text{matching 2}|\text{sub} = \text{air}|\underbrace{\text{matching 1}\text{matching 2}}_{\text{AR}}|\text{sub}. \tag{8.5}$$

Minus filter (notch filter)

The last design we want to discuss is a minus filter, the opposite of a NBP. We can take a QW stack with a small rejection bandwidth. According to equation (7.3) this can be realized with a small refractive index contrast. Alternatively one can also use a Bragg filter, a rugate filter or simply a higher harmonic of a QW.

As an example we can use a QW at 1500 nm with

$$\Delta\lambda\Big|_{\lambda_0} = \frac{4}{\pi} 3\lambda_0 \arcsin\left(\frac{n_H - n_L}{n_H + n_L}\right). \tag{8.6}$$

Since the spectral widths are the same for fundamental and 3rd harmonic $\Delta\nu_{\text{fund}} = \Delta\nu_{\text{3rd harm.}}$ we find for $\Delta\lambda_{\text{3rd}}$

$$\frac{\Delta\lambda_{\text{fund}}}{\lambda^2_{\text{fund}}} = \frac{\Delta\lambda_{\text{3rd}}}{\lambda^2_{\text{3rd}}} \Rightarrow \Delta\lambda_{\text{3rd}} = \frac{\lambda^2_{\text{3rd}}}{\lambda^2_{\text{fund}}} = \frac{1}{9}\Delta\lambda_{\text{fund}} \quad \text{with} \quad \Delta\nu = \frac{\Delta\lambda}{\lambda^2}. \tag{8.7}$$

Furthermore we find that $\Delta\lambda$ decreases for increasing layer thickness d, because thicker layers create finer structures.

9 Helpful formulas

Fresnel equations for oblique incidence

$$\begin{aligned} r_s &= \frac{n_1\cos\varphi - n_2\cos\psi}{n_1\cos\varphi + n_2\cos\psi} \quad \text{and} \quad t_s = \frac{2n_1\cos\varphi}{n_1\cos\varphi + n_2\cos\psi} \\ r_p &= \frac{n_2\cos\varphi - n_1\cos\psi}{n_2\cos\varphi + n_1\cos\psi} \quad \text{and} \quad t_p = \frac{2n_1\cos\varphi}{n_2\cos\varphi + n_1\cos\psi}. \end{aligned} \tag{9.1}$$

System of equation for s-polarized light $\varepsilon = \varepsilon(z)$

$\frac{\mathrm{d}u}{\mathrm{d}z} = \mathrm{i}k_0 v$, $\frac{\mathrm{d}v}{\mathrm{d}z} = \mathrm{i}k_0(\varepsilon - \xi^2)u$ Boundary conditions: $u = 1$, $v = \hat{n}_{\text{sub}}\cos\varphi_s$

reflection coefficients: $t = E_t/E_e$, $r = E_r/E_e$

transmission/reflection coefficients: $t = \frac{2n_0\cos\varphi}{u_0 n_0\cos\varphi + v_0}$, $r = \frac{u_0 n_0\cos\varphi - v_0}{u_0 n_0\cos\varphi + v_0}$

Intensity coefficients: $T = \frac{\mathrm{Re}(\hat{n}_{\text{sub}}\cos\varphi_s)}{n_0\cos\varphi}|t|^2$, $R = |r|^2$.

single film matrix: $\hat{m} = \begin{pmatrix} \cos\delta & -\frac{\mathrm{i}}{n\hat{\cos}\psi}\sin\delta \\ -\mathrm{i}\hat{n}\cos\psi\sin\delta & \cos\delta \end{pmatrix}$ with $\delta = k_0\hat{n}d\cos\psi$

transmission: $t = \frac{2n_0\cos\varphi}{(m_{11} + m_{12}\hat{n}_{\text{sub}}\cos\varphi_s)n_0\cos\varphi + (m_{21} + m_{22}\hat{n}_{\text{sub}}\cos\varphi_s)}$

reflection: $r = \frac{(m_{11} + m_{12}\hat{n}_{\text{sub}}\cos\varphi_s)n_0\cos\varphi - (m_{21} + m_{22}\hat{n}_{\text{sub}}\cos\varphi_s)}{(m_{11} + m_{12}\hat{n}_{\text{sub}}\cos\varphi_s)n_0\cos\varphi + (m_{21} + m_{22}\hat{n}_{\text{sub}}\cos\varphi_s)}$

System of equation for p-polarized light $\varepsilon = \varepsilon(z)$

$\frac{\mathrm{d}u}{\mathrm{d}z} = \mathrm{i}k_0\varepsilon v$, $\frac{\mathrm{d}v}{\mathrm{d}z} = \mathrm{i}k_0\left(1 - \frac{\xi^2}{\varepsilon}\right)u$ Boundary conditions: $u = 1$, $v = \frac{\cos\varphi_s}{\hat{n}_{\text{sub}}}$

reflection coefficients: $t = H_t/H_e$, $r = H_r/H_e$

transmission/reflection coefficients: $t = \frac{2\cos\varphi}{u_0\cos\varphi + n_0 v_0}$, $r = \frac{u_0\cos\varphi - n_0 v_0}{u_0\cos\varphi + n_0 v_0}$

Intensity coefficients: $T = \frac{\mathrm{Re}(\cos\varphi_s/\hat{n}_{\text{sub}})}{\cos\varphi/n_0}|t|^2$, $R = |r|^2$.

single film matrix: $\hat{m} = \begin{pmatrix} \cos\delta & -\frac{\mathrm{i}\hat{n}}{\cos\psi}\sin\delta \\ -\mathrm{i}\cos\psi/\hat{n}\sin\delta & \cos\delta \end{pmatrix}$ with $\delta = k_0\hat{n}d\cos\psi$

transmission: $t = \frac{2n_{\text{sub}}\cos\varphi}{(m_{11}n_{\text{sub}} + m_{12}\cos\varphi_s)\cos\varphi + (m_{21}n_{\text{sub}} + m_{22}\cos\varphi_s)n_0}$

reflection: $r = \frac{(m_{11}n_{\text{sub}} + m_{12}\cos\varphi_s)\cos\varphi - (m_{21}n_{\text{sub}} + m_{22}\cos\varphi_s)n_0}{(m_{11}n_{\text{sub}} + m_{12}\cos\varphi_s)\cos\varphi + (m_{21}n_{\text{sub}} + m_{22}\cos\varphi_s)n_0}$

Reflectance of different QW stacks (no absorption)

$$(\mathrm{LH})^N \qquad R = \left| \frac{n_0 - \left(\frac{n_L}{n_H}\right)^{2N} n_{\mathrm{sub}}}{n_0 + \left(\frac{n_L}{n_H}\right)^{2N} n_{\mathrm{sub}}} \right|^2$$

$$(\mathrm{HL})^N \qquad R = \left| \frac{n_0 - \left(\frac{n_H}{n_L}\right)^{2N} n_{\mathrm{sub}}}{n_0 + \left(\frac{n_H}{n_L}\right)^{2N} n_{\mathrm{sub}}} \right|^2$$

$$\mathrm{H(LH)}^N \qquad R = \left| \frac{n_0 n_{\mathrm{sub}} - \frac{n_H^{2N+1}}{n_L^{2N}}}{n_0 n_{\mathrm{sub}} + \frac{n_H^{2N+1}}{n_L^{2N}}} \right|^2$$

Absorption calculations

Assume $\hat{n} = n + \mathrm{i}\kappa$ and $\varepsilon = \varepsilon_r + \mathrm{i}\varepsilon_i$

Express ε as function of $\hat{n}$: $\varepsilon_r = n^2 - \kappa^2, \quad \varepsilon_i = 2n\kappa$

Express n as function of ε: $n = \frac{1}{\sqrt{2}} \sqrt{\varepsilon_r + \sqrt{\varepsilon_r^2 + \varepsilon_i^2}} \quad \kappa = \frac{\varepsilon_i}{2n}.$

Absorption coefficient: $\alpha = 2\kappa \frac{\omega}{c}, \quad \omega = \frac{2\pi c}{\lambda}.$